Development and implementation of a high-resolution dynamical wall and roof model for ENVI-met

Part 2:
Vegetated walls and roofs

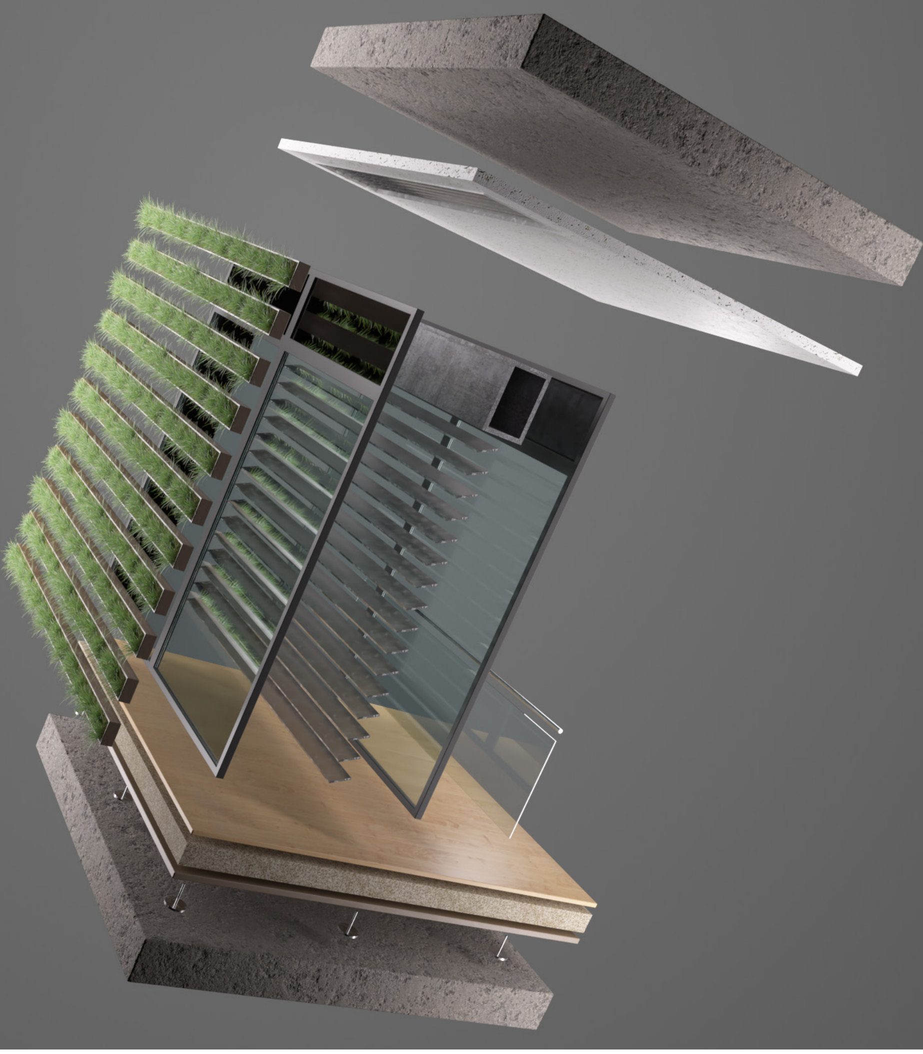

Michael Bruse, Helge Simon and Tim Sinsel
2023

Development and implementation of a high-resolution dynamical wall and roof model for ENVI-met

Part 2: Vegetated walls and roofs

Edition 2023.1

Michael Bruse, Helge Simon and Tim Sinsel

Glossary

Note: Superscripts $\sqcup^{\mathrm{W/L/S}}$ refer to variables at/for the Wall (W), Leaf (L) or Substrate (S) if not noted differently.

Symbol	Description	Unit
Radiation		
$Q^{\mathrm{W/L/S}}_{\mathrm{SW,net}}$	Net absorbed shortwave radiation	$[\mathrm{W\,m^{-2}}]$
$Q^{\mathrm{W/L/S}}_{\mathrm{LW,net}}$	Longwave radiation budget	$[\mathrm{W\,m^{-2}}]$
$Q_{\mathrm{SW,dir}}$	Incoming direct shortwave radiation	$[\mathrm{W\,m^{-2}}]$
$Q_{\mathrm{SW,dif}}$	Incoming diffuse shortwave radiation	$[\mathrm{W\,m^{-2}}]$
$Q_{\mathrm{SW,refl}}$	Incoming reflected shortwave radiation	$[\mathrm{W\,m^{-2}}]$
Q_{LW}	Incoming longwave radiation	$[\mathrm{W\,m^{-2}}]$
$Q^{*}_{\mathrm{SW,dir}}$	Direct shortwave radiation after greening	$[\mathrm{W\,m^{-2}}]$
$Q^{*}_{\mathrm{SW,dif}}$	Diffuse shortwave radiation after greening	$[\mathrm{W\,m^{-2}}]$
$Q^{\mathrm{sum}}_{\mathrm{SW,dif}}$	Sum of incoming diffuse shortwave radiation	$[\mathrm{W\,m^{-2}}]$
Q^{*}_{LW}	Longwave radiation after greening	$[\mathrm{W\,m^{-2}}]$
$Q^{\mathrm{C}}_{\mathrm{SW,dir}}$	Incoming Direct shortwave radiation in the greening center	$[\mathrm{W\,m^{-2}}]$
$Q^{\mathrm{C}}_{\mathrm{SW,dif}}$	Incoming Diffuse shortwave radiation in the greening center	$[\mathrm{W\,m^{-2}}]$
$Q^{\mathrm{C,sec}}_{\mathrm{SW,dif}}$	Secondary Diffuse shortwave radiation created in the greening	$[\mathrm{W\,m^{-2}}]$
$Q_{\mathrm{LW,W}}$	Longwave radiation emitted from the wall or substrate	$[\mathrm{W\,m^{-2}}]$
$Q^{\mathrm{G}}_{\mathrm{LW}}$	Longwave radiation emitted from the green wall system	$[\mathrm{W\,m^{-2}}]$
$Q_{\mathrm{LW,L}}$	Longwave radiation emitted from the leaves	$[\mathrm{W\,m^{-2}}]$
$Q^{\mathrm{C}}_{\mathrm{LW}}$	Longwave radiation emitted in the greening center	$[\mathrm{W\,m^{-2}}]$
$Q^{\mathrm{W}}_{\mathrm{LW,out}}$	Longwave radiation emitted from the building wall	$[\mathrm{W\,m^{-2}}]$
$Q^{\mathrm{ret}}_{\mathrm{SW,dif}}$	Diffuse shortwave radiation returned from wall or substrate	$[\mathrm{W\,m^{-2}}]$
$Q^{\mathrm{C,ret}}_{\mathrm{SW,dif}}$	Diffuse shortwave radiation returned from wall or substrate in the greening center	$[\mathrm{W\,m^{-2}}]$
$Q^{\mathrm{G,ret}}_{\mathrm{SW,dif}}$	Diffuse shortwave radiation returned from greening	$[\mathrm{W\,m^{-2}}]$
$Q^{\mathrm{G,refl}}_{\mathrm{SW,dir}}$	Direct shortwave radiation directly reflected from greening	$[\mathrm{W\,m^{-2}}]$
$Q^{\mathrm{G,refl}}_{\mathrm{SW,dif}}$	Diffuse shortwave radiation directly reflected from greening	$[\mathrm{W\,m^{-2}}]$
$Q^{\mathrm{G,sum}}_{\mathrm{SW,dif}}$	Sum of outgoing diffuse shortwave radiation from greening	$[\mathrm{W\,m^{-2}}]$
Temperatures		
T_{a}	Air temperature in front of GWS	[K]
$T^{\mathrm{C}}_{\mathrm{a}}$	Air temperature within the greening canopy	[K]
T^{*}_{a}	Air temperature behind greening canopy	[K]
T^{**}_{a}	Air temperature within the air gap	[K]
T_{L}	Temperature of leaves in greening canopy	[K]
$T_{\mathrm{W,i}}$	Wall temperature of node i (e.g.$i = 0$ outside)	[K]
$T_{\mathrm{S,i}}$	Temperature of substrate layer i (e.g. $i = 0$ outside)	[K]
$\Delta T_{\mathrm{L,H}}$	Change of air temperature in greening canopy coming from sensible heat flux from the leaves	[K]
$\Delta T_{\mathrm{S*}}$	Change of air temperature in air gap coming from sensible heat flux from the inner substrate layer	[K]
$\Delta T_{\mathrm{W*}}$	Change of air temperature in air gap coming from sensible heat flux from the building wall	[K]
j_H	Heat flux from leaves	$[\mathrm{K\,m\,s^{-1}}]$
Other Microclimate		
$\mathbf{u}$	Tangential Wind speed in front of façade	$[\mathrm{m\,s^{-1}}]$

Symbol	Description	Unit
v^{C}	Wind speed within the greening canopy	$\left[\mathrm{m\,s^{-1}}\right]$
v^{*}	Wind speed behind the greening canopy	$\left[\mathrm{m\,s^{-1}}\right]$
v^{**}	Wind speed in air gap	$\left[\mathrm{m\,s^{-1}}\right]$
q_{a}	Specific humidity of air in front of the GWS	$\left[\mathrm{kg\,kg^{-1}}\right]$
$q_{\mathrm{a}}^{\mathrm{C}}$	Specific humidity of air within the greening canopy	$\left[\mathrm{kg\,kg^{-1}}\right]$
q_{a}^{*}	Specific humidity of air behind the greening canopy	$\left[\mathrm{kg\,kg^{-1}}\right]$
q_{a}^{**}	Specific humidity of air in the air gap	$\left[\mathrm{kg\,kg^{-1}}\right]$
$q_{\mathrm{S,0}}$, $q_{\mathrm{S,6}}$	Specific humidity of outer (0) or inner (6) substrate surface	$\left[\mathrm{kg\,kg^{-1}}\right]$
q^{sat}	Specific humidity at saturation point	$\left[\mathrm{kg\,kg^{-1}}\right]$
$\Delta q_{\mathrm{L,V}}$	Change of specific humidity within the greening canopy	$\left[\mathrm{kg\,kg^{-1}}\right]$
j_S	Vapour flux from substrate directed into greening layer	$\left[\mathrm{kg\,kg^{-1}\,m\,s^{-1}}\right]$
j_E, j_T	Evaporation and transpiration vapour flux from leaves	$\left[\mathrm{kg\,kg^{-1}\,m\,s^{-1}}\right]$
Vegetation		
LAD_{C}	Leaf Area Density of greening layer	$\left[\mathrm{m^2\,m^{-3}}\right]$
LAI	Leaf Area Index	$\left[\mathrm{m^2\,m^{-2}}\right]$
LAI_{C}	Optical Leaf Area Index of greening for direct solar radiation (sun ray's path through the greening canopy)	$\left[\mathrm{m^2\,m^{-2}}\right]$
$LAI_{\mathrm{C,dif}}$	Leaf Area Index of greening for diffuse radiation	$\left[\mathrm{m^2\,m^{-2}}\right]$
Δ_{C}	Thickness of canopy	$[\mathrm{m}]$
r_a	Aerodynamic resistance at leaf surface	$\left[\mathrm{s\,m^{-1}}\right]$
r_s	Stomata resistance of leaf	$\left[\mathrm{s\,m^{-1}}\right]$
α_{L}	Albedo of leaves	$[-]$
φ	Spherical leaf distribution constant = 0.2	$[-]$
γ	Coefficient for leaf angle distribution in greening	$[-]$
ε_{L}	Emissivity of leaves in greening canopy	$[-]$
Other Symbols		
$H^{\mathrm{W/L/S}}$	Sensible heat flux	$\left[\mathrm{W\,m^{-2}}\right]$
$LE^{\mathrm{W/L/S}}$	Latent heat flux	$\left[\mathrm{W\,m^{-2}}\right]$
$G^{\mathrm{W/S}}$	Conduction heat flux	$\left[\mathrm{W\,m^{-2}}\right]$
$\tau_{\mathrm{W/S}}$	Absorption coefficient for shortwave radiation	$[-]$
$\alpha_{\mathrm{W/S}}$	Shortwave albedo	$[-]$
$\varepsilon_{\mathrm{W/S}}$	Longwave emissivity	$[-]$
$\lambda_{\mathrm{W/S}}$	Heat conductivity	$\left[\mathrm{W\,K^{-1}\,m^{-1}}\right]$
β	Angle between façade or roof normal and sun	$[^\circ]$
h_c	Heat transfer coefficient at a surface	$\left[\mathrm{W\,m^{-2}\,K^{-1}}\right]$
ω_{G}	Scaling factor for greening layer	$[-]$
c_{D}	Drag coefficient	$[-]$
z_{D}	Displacement height	$[\mathrm{m}]$
z_0	Roughness length	$[\mathrm{m}]$
f_{M}	Turbulent mixing factor for in-canopy conditions	$[-]$
S_θ	Heat exchange with main atmosphere model	$\left[\mathrm{K\,s^{-1}}\right]$
Δt	Time step length	$[\mathrm{s}]$
$\Delta x, \Delta y, \Delta z$	Grid cell resolutions in x, y, and z direction	$[\mathrm{m}]$
Δ_{W}	Half the thickness of neighbouring model grid cell	$[\mathrm{m}]$
$\Delta_{\mathrm{S}}(X)$	Distance between calculation nodes of substrate X	$[\mathrm{m}]$
Δ_{AG}	Thickness of air gap between substrate and wall	$[\mathrm{m}]$
ζ_w	Watering coefficient of substrate	$[-]$
η	Water content of substrate	$\left[\mathrm{m^3\,m^{-3}}\right]$

Symbol	Description	Unit
η_{fc}	Water content at field capacity of substrate	$\left[\mathrm{m}^3\,\mathrm{m}^{-3}\right]$
η_{wp}	Water content at wilting point of substrate	$\left[\mathrm{m}^3\,\mathrm{m}^{-3}\right]$
Constants		
c_p	Specific heat capacity of air = $1005\,\mathrm{J\,K^{-1}\,kg^{-1}}$	$\left[\mathrm{J\,K^{-1}\,kg^{-1}}\right]$
ρ_a	Density of air at $20\,°\mathrm{C} = 1.29\,\mathrm{kg\,m^{-3}}$	$\left[\mathrm{kg\,m^{-3}}\right]$
κ	Von Karman constant = 0.4	$[-]$
σ_B	Stefan-Boltzmann constant = $5.67 \times 10^{-8}\,\mathrm{W\,m^{-2}\,K^{-4}}$	$\left[\mathrm{W\,m^{-2}\,K^{-4}}\right]$
L	Latent heat of vaporization of water = $2264.705\,\mathrm{kJ\,kg^{-1}}$	$\left[\mathrm{kJ\,kg^{-1}}\right]$

1 Introduction

This paper describes the extension of the ENVI-met Wall and Roof Model (Part 1) with the Green Wall System (GWS), which takes into account vegetated walls and roofs. Vegetated roofs and walls (hereafter only walls) have become an important tool both for green building design and for heat stress mitigation in built-up areas (Perini and Rosasco, 2013). It is therefore important to provide an option for realistic simulation of these specific wall systems in ENVI-met. Figure 1 shows the concept of different possibilities for the definition and modelling of green wall systems and green roofs.

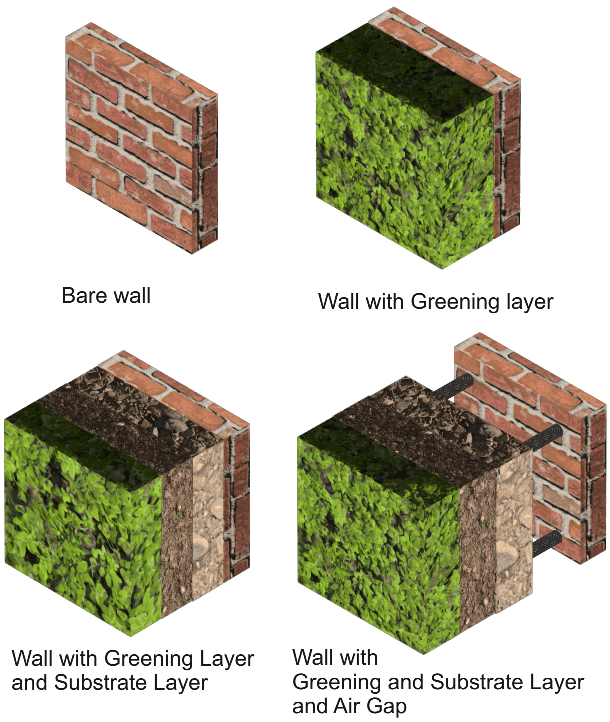

Figure 1: Different possibilities to define and model green walls and roof top greening systems in ENVI-met

The main objective for the modelling of vegetated walls in ENVI-met is to maintain a coherent scheme for the modelling of the wall system, while at the same time taking advantage of the many possibilities offered by the ENVI-met vegetation model. In this way, an efficient numerical scheme can be implemented and the required databases are kept to a minimum.

In the case of green roofs, but also in the case of vegetation elements attached to vertical walls, the substrate in which the vegetation is planted plays an important role in the energy balance of the green wall system. Sometimes the energy exchange with the substrate layer is even more important than the exchange with the vegetation layer planted on it (Gross, 2012; Heusinger and Weber, 2017).

While the modelling of the vegetation layer is conceptually linked to the plant model in ENVI-met, the simulation of the substrate layer is linked to the soil model. The thermal exchange processes that take place in the substrate layer are similar to modelling the base wall material, but the model must take into account the presence of water in the material. In ENVI-met we use the same conceptual model design for the substrate layer as we use to model the soil system.

In the following, the general concept of calculating energy fluxes at building surfaces will be briefly presented in section 3 in order to understand the changes in incoming and outgoing fluxes associated with greening and substrate layers, which will be explained in sections 4 and 5 respectively.

What is missing? An outlook

Although the wall model and the wall greening model already consider a significant number of processes, there are still several tasks to be addressed in future developments. The subsequent list highlights some of the apparent expansions to the current model, but is by no means exhaustive.

Interaction with CO_2 Model: Currently, the greening layer does not provide any feedback to the CO_2 submodel of ENVI-met. Therefore, the uptake or emission of CO_2 does not alter the balance or atmospheric concentration of CO_2. Additionally, the processes in the greening layer are not included in the output of vegetation statistics.

Deposition of Pollutants The greening layer's vegetation is calculated to not be subject to deposition of particulate or gaseous pollutants. While the presence of facade and roof greening may influence pollutant dispersion through changes in the wind field, such effects come from variations in the roughness of the building walls or through changes in the thermal stratification, not through direct uptake of pollutants.

Advanced Watering Control The availability of water is crucial for the functioning and monitoring of green roofs and facades. As the substrate available is generally limited and exposes to high solar radiation and wind, an additional watering system is usually necessary. In the latest version, a watering coefficient can be set for substrate-bound green systems. As demonstrated in this paper, for GWS involving substrates outside of the greening system itself, such as ground-based climbing plants, unrestricted access to water is assumed. However, for more individualised watering strategies, a building-oriented watering concept would be more realistic and should be considered in future versions.

2 Definition of the Green Wall System

The selection of greenery for façade or roof greening is outlined by a newly created 'Facade/Roof Greening' information layer within the ENVI-met database system. The following items are defined in the new database section:

- Relational link to a Simple Plant database item (only few items such as albedo, leaf type, tree calendar etc. are used)
- Relational link to three items from Soil database, if a substrate is used
- Δ_{C}: Thickness of vegetation layer / canopy
- LAI: Leaf Area Index of the vegetation layer
- Δ_{S}: Thickness of the three substrate layers, if a substrate is used
- ζ_w: Watering coefficient, if a substrate is used
- γ: Leaf angle distribution
- Δ_{AG}: Air gap size between substrate and building wall, if a substrate layer is used and if an air gap exists

Differing from other single-standing vegetation in ENVI-met we use the Leaf Area Index (LAI) instead of the Leaf Area Density (LAD) to define the amount of foliage of the vegetation layer.

For the relatively thin vegetation layers, LAI is more understandable and straight forward to use as it can also be understood as a cover coefficient for $LAI < 1$ (compare Fig. 2).

Moreover, as LAD is defined per cubic metre, extrapolating the leaf density in the thin vegetation layer to a larger volume would result in extremely high LAD values, which could be confusing when compared to typical values observed in trees or similar structures. For example, a typical average LAI of 2.0 in a 30 cm vegetation layer of *Tricuspidata spec.* would numerically equal a LAD of $2.0/0.3 = 6.66$, which would not be in line with common values observed in trees.

Figure 2: Example for different approximated LAI indices and coverages for a wall-climbing *Tricuspidata spec.*

Water management of the green wall system

The precise depiction of water availability is imperative for modelling vegetation transpiration and its cooling capacity. For common ground vegetation, the hydrological part of the ENVI-met soil model provides continuous information on the water content within the root zone of the plants and also balances the transpired water with the water content of the soil.

For vegetated walls and roofs in ENVI-met, it is assumed that a managed irrigation system is available to regulate and provide water to the plants, either on the roof or at the facade. As such, an adjustable watering coefficient ζ_w is defined, with a range from 0 (indicating dry conditions) to 1 (indicating moist conditions), to describe the water accessibility for plants. Furthermore, depending on the design of the green wall system, a distinction is made between different types of vegetation:

- GWS without a substrate layer (e.g. climbing plants): A constant and sufficient water supply is assumed (ζ_w=1)
- GWS with substrate layer (e.g. living wall system): The watering coefficient can be defined for each greening system as a constant factor that defines both the water content of the substrate and the water supply of the connected plants (ζ_w=[0..1])

The effect of the watering coefficient will be discussed in later sections of this paper.

3 Energy balance calculation at the building surface

As the existence of a greening layer significantly alters the energy balance of the external wall or roof, we will provide a brief overview of its basic components in this section. This is merely a summary of the building wall model. For a comprehensive depiction of the system and the consequent response of the entire wall system, please refer to Part 1 of this paper, as well as the Ph. D. thesis of Huttner (2012) and Simon (2016).

3.1 Energy balance of the outside facade

The energy balance for the outside facade of a wall or roof is calculated based on the incoming and outgoing energy fluxes:

$$Q^{\mathrm{W}}_{\mathrm{SW,net}} + Q^{\mathrm{W}}_{\mathrm{LW,net}} - H^{\mathrm{W}} - LE^{\mathrm{W}} - G^{\mathrm{W}} = 0 \quad (3.1)$$

It consists of received and absorbed shortwave radiation ($Q^{\mathrm{W}}_{\mathrm{SW,net}}$), longwave radiation budget ($Q^{\mathrm{W}}_{\mathrm{LW,net}}$), sensible heat flux ($H^{\mathrm{W}}$), latent heat flux ($LE^{\mathrm{W}}$) and conduction heat flux (G^{W}) discussed in the following sections.

3.1.1 Radiative Fluxes

Incoming shortwave radiation consists of the direct component ($Q_{\mathrm{SW,dir}}$), which is reduced by the Lambert law (β as angle between façade normal and sun position), the diffuse component ($Q_{\mathrm{SW,dif}}$) and the reflected radiation received from the environment ($Q_{\mathrm{SW,refl}}$), which are summed up and multiplied with the absorption value (τ_{W}) of the wall surface material (Eq. 3.2).

$$Q^{\mathrm{W}}_{\mathrm{SW,net}} = \tau_{\mathrm{W}} \cdot \Big(\cos(\beta) \cdot Q_{\mathrm{SW,dir}} + Q_{\mathrm{SW,dif}} + Q_{\mathrm{SW,refl}}\Big) \quad (3.2)$$

The net longwave radiation budget ($Q^{\mathrm{W}}_{\mathrm{LW,net}}$) is determined by the incoming (Q_{LW}) and outgoing longwave radiation. This is calculated using the emissivity ε_{W}, surface temperature $T_{\mathrm{W},0}$, and Stefan-Boltzmann constant ($\sigma = 5.67 \cdot 10^{-8}$) of the wall material.

$$Q^{\mathrm{W}}_{\mathrm{LW,net}} = Q_{\mathrm{LW}} - \Big((1-\varepsilon_{\mathrm{W}}) \cdot Q_{\mathrm{LW}} + \sigma_B \cdot \varepsilon_{\mathrm{W}} \cdot T^4_{\mathrm{W},0}\Big) \quad (3.3)$$

3.1.2 Turbulent Fluxes

The **Sensible heat flux** H^{W} is calculated based on the heat transfer coefficient between the wall and the air (h^{W}_c) and the temperature difference between wall outer surface $T_{\mathrm{W},0}$ and the air temperature T_{a} (Eq. 3.4):

$$H^{\mathrm{W}} = h^{\mathrm{W}}_c \cdot (T_{\mathrm{W},0} - T_{\mathrm{a}}) \quad (3.4)$$

The heat transfer coefficient, h^{W}_c, between the wall and the surrounding air is calculated using either DIN 6946 (default) or Monin-Obhukov (see Section 2.2.2 in Part 1 of this paper) on the basis of the tangential wind speed located in front of the greening, $\mathbf{u}$.

Latent heat flux LE^{W} at the wall is set to 0 in case of bare walls without greening and substrate (Eq. 3.5).

$$LE^{\mathrm{W}} = 0 \quad (3.5)$$

3.1.3 Heat conduction into/from the wall

The Conduction heat flux (G^{W}) is determined by the temperature difference between wall nodes $T_{\mathrm{W},0}$ as outside node and $T_{\mathrm{W},1}$ as first inside node (Node 1 of the wall system in Part 1) as well as heat conductivity ($\lambda_{\mathrm{W,A}}$) and thickness ($\Delta\mathrm{A}$) of the wall material A:

$$G^{\mathrm{W}} = \frac{\lambda_{\mathrm{W,A}}}{0.5 \cdot \Delta\mathrm{A} \cdot (T_{\mathrm{W},0} - T_{\mathrm{W},1})} \quad (3.6)$$

3.2 Outgoing fluxes from the wall

The fluxes coming from the wall are not an integral part of the energy system of the wall, but provide the necessary feedback to the main model. These comprise the shortwave radiation reflected from the wall, thermal radiation from the wall and turbulent fluxes of heat and vapour.

In the case of bare walls discussed in this section, these fluxes are directly linked to the main model through source terms in the prediction equations for temperature and humidity. Radiative fluxes are considered when using the IVS algorithm (Simon et al., 2021) to simulate radiative exchanges between various surfaces.

If a green system is affixed to the wall, the outgoing fluxes from the wall will not directly interact with the atmosphere but instead serve as secondary inputs for the GWS (refer to later sections).

The **outgoing radiative fluxes** (shortwave $Q^{\mathrm{ret}}_{\mathrm{SW,dif}}$ and longwave $Q^{\mathrm{W}}_{\mathrm{LW,out}}$) from the wall back to the atmosphere (in the case of a bare wall) are calculated as:

$$Q_{\mathrm{SW,dif}}^{\mathrm{ret}} = \alpha_{\mathrm{W}} \cdot \left(Q_{\mathrm{SW,dir}} \cdot \cos(\beta) + Q_{\mathrm{SW,dif}} + Q_{\mathrm{SW,refl}}\right) \tag{3.7}$$

Note, that the outgoing shortwave radiation is handled as diffuse radiation, hence no directed reflection is supported.

The outgoing longwave flux can be written as:

$$Q_{\mathrm{LW,out}}^{\mathrm{W}} = (1 - \varepsilon_{\mathrm{W}}) \cdot Q_{\mathrm{LW}} + \sigma_B \cdot \varepsilon_{\mathrm{W}} \cdot T_{\mathrm{W},0}^4 \tag{3.8}$$

The outgoing flux of **sensible heat** is linked directly with the ENVI-met main atmosphere model as discussed in Section 6, p. 17.

4 Modelling the Greening Layer

The simplest way to implement facade or roof greening is by using climbing or hanging plants to create a green layer in front of the building wall or roof. In the following section, we'll provide a general overview of the facade greening model and its effects on the building's microclimate conditions behind or below the vegetation layer. In later sections, we'll expand on this concept by introducing a substrate layer for more complex greening systems.

4.1 General model concept

If a green layer exists, the energy fluxes to and from the wall will be altered. The following section presents the distinct handling of direct and diffuse shortwave radiation, longwave radiation, as well as other parameters, such as sensible and latent heat flux, wind speed, air temperature, and specific humidity.

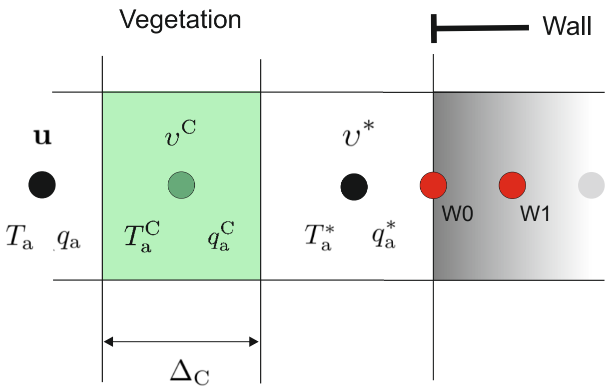

Figure 3: Concept diagram of a green wall system with greening layer including the main prognostic variables

Figure 3 illustrates the general concept of a building wall with an adjacent vegetation layer. In particular, the figure illustrates the concept of naming the main variables at the interface with the atmosphere (tangential wind speed $\mathbf{u}$, air temperature T_{a}, Specific humidity q_{a}), their state within the vegetation layer ($\upsilon_{\mathrm{a}}^{\mathrm{C}}$, $T_{\mathrm{a}}^{\mathrm{C}}$, $q_{\mathrm{a}}^{\mathrm{C}}$) and their modified counterparts on the building side ($\upsilon_{\mathrm{a}}^{*}$, T_{a}^{*}, q_{a}^{*}). Nodes $W0$ and $W1$ represent the two outermost calculation points of the seven points in the dynamic wall model.

4.2 Modification of radiative fluxes

Both shortwave and longwave radiation are modified as they pass through the vegetation layer. On the one hand, the transmission and subsequent absorption processes at the leaves of the GWS determine the leaf temperature and other plant-related processes in the greening layer. On the other hand, reflection, scattering and absorption modify the amount and distribution of radiation received by the building wall behind the vegetation layer. Both effects are discussed in the following sections.

4.2.1 Direct shortwave radiation

The treatment of direct shortwave radiation for the Green Wall System follows the calculations of the Advanced Canopy Radiation Transfer (ACRT) module (Goudriaan, 1977; Pedruzo-Bagazgoitia et al., 2017; Simon et al., 2020; Spitters et al., 1986), which has been added to the ENVI-met radiation/vegetation model with V5. Figure 4 gives a schematic overview of the incoming and outgoing shortwave fluxes in the GWS.

The primary extinction of direct radiation is modelled using an extinction coefficient (k_{dirbl}) that depends on the angle between the incoming direct solar radiation and the surface normal:

$$k_{\mathrm{dirbl}} = \frac{0.5}{\sin(\beta)} \tag{4.1}$$

As the primary extinction of direct radiation only considers the pure extinction of direct radiation, leaves are considered visually black, neither transmitting nor reflecting, only absorbing direct radiation.

The transmission factor for the primary extinction of direct radiation ($f_{\mathrm{dir,pri}}$) within the foliage is then calculated by

$$f_{\mathrm{dir,pri}} = (1 - \rho_{dir}) \cdot (1 - \varphi) \cdot e^{-(k_{\mathrm{dirbl}} \cdot LAI_{\mathrm{C}})} \tag{4.2}$$

with $\varphi = 0.2$ as a constant for a spherical leaf distribution and the optical Leaf Area Index LAI_{C} calculated for the path of direct radiation through the canopy of the greening layer as a function of the canopy thickness Δ_{C} and the angle of the sun to the wall normal β:

$$LAI_{\mathrm{C}} = LAD_{\mathrm{C}} \cdot \Delta_{\mathrm{C}} \cdot \frac{1}{\cos(\beta)} \tag{4.3}$$

Since a fraction of the incident direct radiation is reflected and does not enter the canopy, equation 4.2 requires a reflection coefficient ρ_{dir} for the outside of the canopy:

$$\rho_{\mathrm{dir}} = \rho \frac{2}{1 + 1.6 \sin(\beta)} \tag{4.4}$$

Here, ρ_{dir} is defined as a function of the solar angle β and a simple reflection coefficient ρ (Eq. 4.5) ,

$$\rho = \frac{1 - \sqrt{1 - \varphi}}{1 + \sqrt{1 - \varphi}} \tag{4.5}$$

Modified direct radiation behind the greening canopy $Q^{*}_{\mathrm{SW,dir}}$

The modified direct shortwave radiation behind the greening $Q^{*}_{\mathrm{SW,dir}}$ is calculated by multiplying the incoming shortwave radiation from the main model $Q_{\mathrm{SW,dir}}$ by the defined extinction factor for direct radiation $f_{\mathrm{dir,pri}}$ given by (4.2):

$$Q^{*}_{\mathrm{SW,dir}} = Q_{\mathrm{SW,dir}} \cdot f_{\mathrm{dir,pri}} \tag{4.6}$$

Outgoing reflected direct shortwave radiation $Q^{\mathrm{G,refl}}_{\mathrm{SW,dir}}$

The counterpart of the incoming direct shortwave radiation that is not transmitted by the foliage is reflected outwards $Q^{\mathrm{G,refl}}_{\mathrm{SW,refl}}$ using the albedo of the leaves α_{L}:

$$Q^{\mathrm{G,refl}}_{\mathrm{SW,dir}} = Q_{\mathrm{SW,dir}} \cdot (1 - f_{\mathrm{dir,pri}}) \cdot \alpha_{\mathrm{L}} \tag{4.7}$$

In-Canopy direct shortwave radiation $Q^{C}_{\mathrm{SW,dir}}$

For direct shortwave radiation within the canopy, the use of $f_{\mathrm{dir,pri}}$ is not feasible due to its accounting for the entire distance through the greening layer. Thus, we calculate the extinction factor for the midpoint of the greening layer ($f^{c}_{\mathrm{dir,pri}}$) using Equation (4.2), with only half of LAI_{C} being utilized.

$$f^{c}_{\mathrm{dir,pri}} = (1 - \rho_{\mathrm{dir}}) \cdot (1 - \varphi) \cdot e^{-(k_{\mathrm{dirbl}} \cdot 0.5 LAI_{\mathrm{c,dir}})} \tag{4.8}$$

The resulting direct shortwave radiation within the canopy $Q^{C}_{\mathrm{SW,dir}}$ is then calculated by:

$$Q^{C}_{\mathrm{SW,dir}} = Q_{\mathrm{SW,dir}} \cdot f^{c}_{\mathrm{dir,pri}} \tag{4.9}$$

4.2.2 Diffuse shortwave radiation

Diffuse shortwave radiation is computed in accordance with ACRT module equations. The extinction coefficient for diffuse radiation, k_{dif}, is analogous to its direct counterpart, but since diffuse radiation is assumed to be isotropic, the solar angle dependence is neglected and replaced by a constant factor of 0.8:

$$k_{\mathrm{dif}} = 0.8 \cdot \sqrt{1 - \varphi} \tag{4.10}$$

The transmission factor for diffuse shortwave radiation $f_{\mathrm{dif,pri}}$ is then calculated with:

$$f_{\mathrm{dif,pri}} = (1 - \rho) \cdot e^{-(k_{\mathrm{dif}} \cdot LAI_{\mathrm{C,dif}})} \tag{4.11}$$

where the Leaf Area Index $LAI_{\mathrm{C,dif}}$ is also defined without any sun angle dependency, hence the sun path length

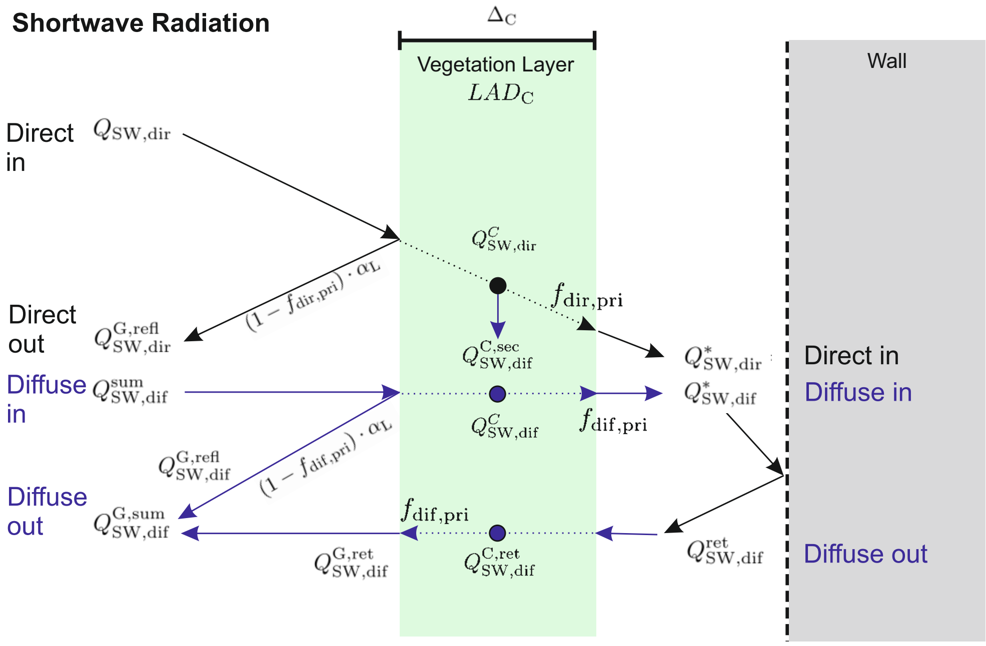

Figure 4: Schematic overview showing the incoming and outgoing shortwave radiation fluxes for a green wall system without substrate layer

through the canopy corresponds with the thickness of the greening layer Δ_C:

$$LAI_{C,dif} = LAD_C \cdot \Delta_C \tag{4.12}$$

The incoming diffuse radiation in the greening module ($Q^{sum}_{SW,dif}$) is treated as the sum of diffuse and reflected shortwave radiation provided by the main atmospheric model:

$$Q^{sum}_{SW,dif} = Q_{SW,dif} + Q_{SW,refl} \tag{4.13}$$

Modified diffuse radiation behind the greening canopy $Q^*_{SW,dif}$

The amount of diffuse shortwave radiation behind the greening and hence after the extinction is determined by using the extinction coefficient $f_{dif,pri}$ (eq. 4.14).

$$Q^*_{SW,dif} = Q^{sum}_{SW,dif} \cdot f_{dif,pri} \tag{4.14}$$

Outgoing diffuse shortwave radiation $Q^{G,sum}_{SW,dif}$

The calculation of the outgoing diffuse radiation is more complex than its direct counterpart because it also needs to consider the potential reflection of shortwave radiation at the building facade. Therefore, the outgoing diffuse shortwave radiation can be written as:

$$Q^{G,sum}_{SW,dif} = Q^{G,refl}_{SW,dif} + Q^{G,ret}_{SW,dif} \tag{4.15}$$

The term $Q^{G,refl}_{SW,dif}$ represents the diffuse radiation that is scattered directly outside the greening layer. The second term on the RHS, $Q^{G,ret}_{SW,dif}$, describes the shortwave radiation that passes through the greening layer, reflects off the building wall, and passes through the vegetation layer again (returning shortwave radiation).

For the diffuse radiation immediately reflected at the outside of the canopy, the formulation is similar to the direct component in (4.7), but it uses the sun angle-independent formulation of the reflection coefficient ρ provided in (4.5).

$$Q^{G,refl}_{SW,dif} = Q^*_{SW,refl} \cdot (1 - f_{dif,pri}) \cdot \alpha_L \tag{4.16}$$

To compute the returning component, we calculate the reflection of both direct and diffuse radiation that has passed through the greening layer using the albedo of the wall (α_W):

$$Q^{ret}_{SW,dif} = \alpha_W \cdot \left(Q^*_{SW,dir} + Q^*_{SW,dif}\right) \cdot \tag{4.17}$$

To calculate the reflection of radiation behind the greenery, we treat the direct and diffuse components equally, without considering sun angle dependency in the direct component. This is due to our assumption that the original sun direction is no longer valid through scattering and multiple reflections.

The reflected radiation amount is then reduced by the extinction coefficient of diffuse radiation when transmitted through the greening canopy using the previously defined extinction coefficient. Therefore, we can express the shortwave radiation leaving the green wall system as:

$$Q^{\mathrm{G,ret}}_{\mathrm{SW,dif}} = Q^{\mathrm{ret}}_{\mathrm{SW,dif}} \cdot f_{\mathrm{dif,pri}} \tag{4.18}$$

In-Canopy diffuse shortwave radiation $Q^{C}_{\mathrm{SW,dif}}$

The diffuse shortwave radiation in the center of the green canopy is composed out of three components:

1. Transmitted incoming diffuse radiation $Q^{C}_{\mathrm{SW,dif}}$
2. Transmitted returning diffuse radiation reflected from the wall $Q^{\mathrm{C,ret}}_{\mathrm{SW,dif}}$
3. Additional diffuse radiation originating from scattered direct radiation $Q^{\mathrm{C,sec}}_{\mathrm{SW,dif}}$

Therefore, we can calculate the overall level of scattered radiation as

$$Q^{C}_{\mathrm{SW,dif}} = Q^{C}_{\mathrm{SW,dif}} + Q^{\mathrm{C,ret}}_{\mathrm{SW,dif}} + Q^{\mathrm{C,sec}}_{\mathrm{SW,dif}} \tag{4.19}$$

For the computation of component (1), the principle used for the direct component applies to the transmitted incoming diffuse shortwave radiation as well (refer to equation 4.11). When calculating the extinction factor, we consider half of the $LAI_{\mathrm{c,dif}}$ after equation (4.12) to represent the value at the center of the greening layer:

$$f^{c}_{\mathrm{dif,pri}} = (1-\rho) \cdot e^{-(k_{\mathrm{dif}} \cdot 0.5 LAI_{\mathrm{c,dif}})} \tag{4.20}$$

The incoming diffuse radiation in the canopy center is then

$$Q^{C}_{\mathrm{SW,dif}} = Q_{\mathrm{SW,dif}} \cdot f^{c}_{\mathrm{dif,pri}} \tag{4.21}$$

For the estimation of the **returning** diffuse radiation (2), the required extinction coefficient $f^{c}_{\mathrm{dif,pri}}$ is identical to the value for the incoming radiation (4.20), as the same amount of vegetation is passed. So we can calculate the returning reflected shortwave radiation as:

$$Q^{\mathrm{C,ret}}_{\mathrm{SW,dif}} = Q^{\mathrm{ret}}_{\mathrm{SW,dif}} \cdot f^{c}_{\mathrm{dif,pri}} \tag{4.22}$$

As the third component (3) in the diffuse radiation spectrum, it is necessary to consider a source of *secondary diffuse shortwave radiation*, which is produced by the scattering of direct shortwave radiation within the canopy layer.

This secondary source of diffuse radiation is located in the centre of the vegetation layer and can be expressed as follows:

$$Q^{\mathrm{C,sec}}_{\mathrm{SW,dif}} = Q_{\mathrm{SW,dir}} \cdot f^{c}_{\mathrm{sec}} - Q_{\mathrm{SW,dir}} \cdot f^{c}_{dir,pri} \tag{4.23}$$

(compare Simon et al., 2020, eqs. 7 – 11).

To solve the equation, a modified transmission factor f^{c}_{sec} is defined as

$$f^{c}_{\mathrm{sec}} = (1-\rho_{\mathrm{dir}}) \cdot e^{-(k_{\mathrm{dir}} \cdot 0.5 LAI_{\mathrm{c,dir}})} \tag{4.24}$$

using k_{dir} as a modification of the direct shortwave radiation extinction coefficient k_{dirbl} (see eq. 4.1):

$$k_{\mathrm{dir}} = k_{\mathrm{dirbl}} \cdot \sqrt{1-\varphi} \tag{4.25}$$

4.2.3 Longwave radiation

Like shortwave radiation, longwave thermal radiation is also modified while passing through the vegetation layer. Figure 5 illustrates the concept of longwave radiation fluxes.

When modelling longwave radiation within and behind the greening, transmission factors are not explicitly considered. Instead, a parameter known as coefficient P (with a range from 0 to 1) is utilised to ascertain the likelihood of longwave radiation reaching a leaf within the greening canopy (Cescatti, 1997; Nilson, 1971). As P approaches 1, more and more of the incoming longwave radiation is replaced by the longwave radiation emitted by the leaves of the canopy.

The likelihood of hitting a leaf P as the radiation passes through a canopy layer of density LAD and thickness Δ_{C} can be written as

$$P = 1 - e^{-\gamma \cdot LAD \cdot \Delta_{\mathrm{C}}} \tag{4.26}$$

using the leaf angle distribution γ, as specified by the user, with values ranging between 0 for horizontally positioned leaves and 1 for vertically arranged leaves (see Figure 6).

Modified longwave radiation behind the greening canopy Q^{*}_{LW}

Following the probability concept explained previously, the modification of longwave radiation behind the greening layer Q^{*}_{LW} can be determined by calculating the weighted average of the incoming longwave radiation Q_{LW} and the longwave radiation that the leaves emit $Q_{\mathrm{LW,L}}$:

$$Q^{*}_{\mathrm{LW}} = (1-P) \cdot Q_{\mathrm{LW}} + P \cdot Q_{\mathrm{LW,L}} \tag{4.27}$$

with the longwave radiation emitted from the leaves calculated as:

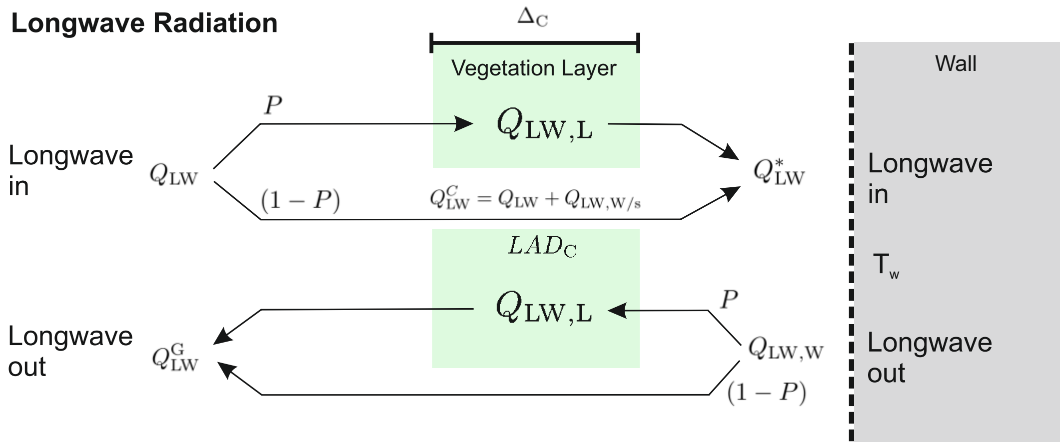

Figure 5: Schematic overview showing the incoming and outgoing longwave radiation fluxes for a green wall system without substrate layer

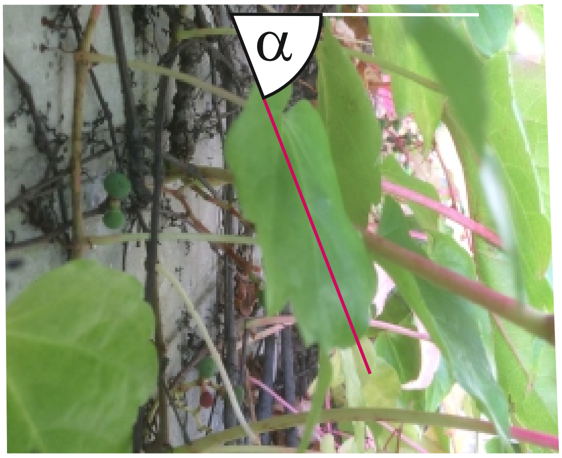

Figure 6: Definition of leaf angle $\gamma = \sin(\alpha)$ for the calculation of longwave radiative transfer with $\gamma = 0$ for horizontal to $\gamma = 1$ for vertical leaves

$$Q_{LW,L} = (1 - \varepsilon_L) \cdot Q_{LW} + \sigma \cdot \varepsilon_L \cdot {T_L}^4 \tag{4.28}$$

Outgoing longwave radiation Q^G_{LW}

The total outgoing longwave radiation from the entire facade (Q^G_{LW}) follows the same concept as that of the emitted longwave radiation of the leaves $Q_{LW,L}$ and emission of the wall or, if present, substrate layer ($Q_{LW,W/S}$).

$$Q^G_{LW} = P \cdot Q_{LW,L} + (1 - P) \cdot Q_{LW,W/S} \tag{4.29}$$

The longwave emission of the wall or substrate layer is given by

$$Q_{LW,W/S} = (1 - \varepsilon_{W/S}) \cdot Q^*_{LW} + \sigma_B \cdot \varepsilon_{W/S} \cdot T^4_{W/S,0} \tag{4.30}$$

with $\varepsilon_{W/S}$ being the emissivity of the wall or substrate and $T_{W/S,0}$ its surface temperature.

In-Canopy longwave radiation Q^C_{LW}

The leaves within the greening layer receive longwave radiation from two sources: the atmosphere and the building wall or substrate layer. To compute the radiation in the layer's center, both fluxes are combined.

$$Q^C_{LW} = Q_{LW} + Q_{LW,W/s} \tag{4.31}$$

4.3 Modification of Wind Speed, Air Temperature and Specific Humidity

The meteorological conditions within the relatively thin vegetation layer are defined by the atmospheric conditions on the outside and the conditions generated by the building wall or substrate on the inside as boundary conditions. Besides, the temperature and vapor flux of the leaves also modify the state of the air inside the canopy.

As it is not feasible to explicitly simulate the atmospheric processes within the vegetation canopy, including the advective exchange with other facade elements, a simple algorithm is required to estimate the microclimatic conditions within the canopy.

In general terms, two extreme situations can be envisioned that define the mixing conditions in the green canopy layer.

- **Non-Mixed State:** In the non-mixed state, the wind speed within the canopy is low so that the leaves and the attached wall or substrate have a significant impact on the in-canopy meteorological values.

- **Optimal-Mixed State:** The optimal-mixed state is characterized by relatively high wind speeds. Under these conditions, the air exchange rate within the canopy and with the air around the building is high, and the in-canopy conditions are mainly the same as the microclimate conditions in front of the facade.

In most cases, a mixture between these two extreme conditions will be observed. Hence, we need to define and calculate a mixing factor depending on the local wind conditions.

4.3.1 In-canopy Wind Speed v^{C} and Mixing Factor f_M

The in-canopy wind speed is required for the calculation of the leaf temperature T_L^C and the mixing factor f_M mentioned above.

In-canopy Wind Speed

We define the in-canopy wind speed as the average of the tangential wind speed $\mathbf{u}$ in front of the greening layer and the to-be-defined adjusted wind speed behind it v^*:

$$v^{\mathrm{C}} = 0.5 \cdot (\mathbf{u} + v^*) \tag{4.32}$$

This approach was chosen to reflect the situation that, depending on the density of the canopy given by the greening weight (see below), the greening layer is patchwork of green and non-green sections. Through the non-green section, the wind can flow more or less freely and also influence leaves in the inner parts of the green patches. Hence, a strict application of the drag concept as given by (4.35) was considered less realistic in the inner parts of the greening layer rather than averaging the two boundary conditions.

The wind speed behind the greening v^* (or the modified wind speed in front of the facade) is calculated by reducing the wind speed in front of the greening using a greening weight (ω_{G}) and a drag coefficient (c_{D}):

$$v^* = (1 - \omega_{\mathrm{G}}) \cdot \mathbf{u} + \omega_{\mathrm{G}} \cdot c_{\mathrm{D}} \cdot \mathbf{u} \tag{4.33}$$

ω_{G} is a general scaling factor related to the Leaf Area Density of the greening layer LAD_{C} :

$$\omega_{\mathrm{G}} = 1 - e^{-LAD_{\mathrm{C}}} \tag{4.34}$$

The drag coefficient c_{D} for vegetation takes the von-Karman constant ($\kappa = 0.4$), canopy roughness length (z_0), and wall displacement height (z_{d}) into account:

$$c_{\mathrm{D}} = \sqrt{\frac{\kappa^2}{\left(\frac{\ln(\Delta_{\mathrm{W}} + z_{\mathrm{d}})}{z_0}\right)^2}} \tag{4.35}$$

Here, z_0 as the roughness of the greening layer depends on greening canopy thickness (Δ_{C}):

$$z_0 = 0.131 \cdot \Delta_{\mathrm{C}}{}^{0.997} \tag{4.36}$$

The displacement height z_{d} of the wall depends on the distance to the next atmospheric calculation node Δ_{W}, which is half the grid cell size for centered variables (Balick et al., 1981; Oosterlee, 2013; Sailor, 2008):

$$z_{\mathrm{d}} = 0.701 \cdot \Delta_{\mathrm{W}}{}^{0.979} \tag{4.37}$$

Mixing Factor

The estimated wind speed inside the canopy v^{C} can then used to define the dimensionless turbulent mixing factor f_{M} with:

$$f_{\mathrm{M}} = v_{\mathrm{C}} - 0.5 \tag{4.38}$$

Eq. 4.38 has a lower limit of 0 and an upper limit of 1:

$$f_{\mathrm{M}} \equiv \begin{cases} 0 & ; f_{\mathrm{M}} < 0 \\ 1 & ; f_{\mathrm{M}} > 1 \end{cases} \tag{4.39}$$

f_{M} determines the weight of the conditions in front of and within the canopy for the calculation of air temperature and specific humidity.

A high value for f_{M} accounts for high wind speeds and a strong mixing effect of outdoor conditions with the canopy, while a low f_{M} stands for low wind speeds and hence sparse mixing with a higher weight for in-canopy conditions.

4.3.2 In-canopy Air Temperature $T_{\mathrm{a}}^{\mathrm{C}}$

By applying the mixing factor f_{M}, the air temperature within the canopy, $T_{\mathrm{a}}^{\mathrm{C}}$, can be computed utilizing both the air temperature in front of the greening, T_{a}, and an air temperature altered by the temperature change term, $\Delta T_{\mathrm{L,H}}$, representing the temperature flux from the leaves in the greening.

$$\begin{aligned} T_{\mathrm{a}}^{\mathrm{C}} = {} & f_{\mathrm{M}} \cdot T_{\mathrm{a}} + \\ & (1 - f_{\mathrm{M}}) \cdot \Big(\omega_{\mathrm{G}} \cdot (T_{\mathrm{a}} + \Delta T_{\mathrm{L,H}}) + (1 - \omega_{\mathrm{G}}) \cdot T_{\mathrm{a}}\Big) \end{aligned} \tag{4.40}$$

with the greening scaling factor ω_{G} as introduced in Eq. 4.34.

The vegetation induced temperature change $\Delta T_{\mathrm{L,H}}$ depends on the sensible heat flux of greenery j_{H} (see eq. 4.54) and the time step length Δt of the simulation:

$$\Delta T_{\mathrm{L,H}} = j_{\mathrm{H}} \cdot \Delta t \cdot LAD^{*} \tag{4.41}$$

Finally, LAD^{*} is a scaled Leaf Area Density taking into account that the relatively thin greening layer only covers a smaller faction of the model grid cell. The definition of LAD^{*} depends on the orientation of the considered wall:

$$LAD^{*} = LAD \cdot \frac{1}{\Delta x \Delta y \Delta z} \cdot \begin{cases} \Delta y \Delta z \Delta_{\mathrm{C}} & \text{;X-Walls} \\ \Delta x \Delta z \Delta_{\mathrm{C}} & \text{;Y-Walls} \\ \Delta x \Delta y \Delta_{\mathrm{C}} & \text{;Roofs/ Z-Walls} \end{cases} \tag{4.42}$$

with Δx, Δy and Δz being the size of the main model grid.

4.3.3 In-canopy Specific Humidity $q_{\mathrm{a}}^{\mathrm{C}}$

The calculation of the specific humidity within the canopy is analogously to the concept presented for the in-canopy air temperature.

The in-canopy specific humidity is defined as a mixture between the air humidity q_{a} in front of the greening and a change term:

$$q_{\mathrm{a}}^{\mathrm{C}} = f_{\mathrm{M}} \cdot q_{\mathrm{a}} + (1 - f_{\mathrm{M}}) \cdot \Big(\omega_{\mathrm{G}} \cdot (q_{\mathrm{a}} + \Delta q_{\mathrm{L,V}})(1 - \omega_{\mathrm{G}}) \cdot q_{\mathrm{a}} \Big) \tag{4.43}$$

Like for the temperature, we define a change term for the specific humidity, which depends on the evaporation j_{E} and transpiration (j_{T}) fluxes of the leaves:

$$\Delta q_{\mathrm{L,V}} = (j_{\mathrm{E}} + j_{\mathrm{T}}) \cdot \Delta t \cdot LAD^{*} \tag{4.44}$$

The calculation of the evaporation and transpiration fluxes is discussed in the next section.

If a substrate layer is present and the topmost layer of the substrate is capable of evaporating water, an extra water flow denoted as j_{S} contributes to the humidity inside the plant canopy (refer to equation 5.17, page 15).

$$\Delta q_{\mathrm{L,V}} = (j_{\mathrm{E}} + j_{\mathrm{T}}) \cdot LAD^{*} \cdot \Delta t + j_{\mathrm{S}} \cdot A^{*} \cdot \Delta t \tag{4.45}$$

The scaling factor A^{*} relates the substrate surface area to the volume of the vegetation layer with

$$A^{*} = \frac{A}{A \cdot \Delta_{\mathrm{C}}} \text{ with } A = \begin{cases} \Delta y \Delta z & \text{;X-Walls} \\ \Delta x \Delta z & \text{;Y-Walls} \\ \Delta x \Delta y & \text{;Roofs/ Z-Walls} \end{cases} \tag{4.46}$$

4.3.4 Temperature T_{a}^{*} and Specific Humidity q_{a}^{*} behind the greening layer

For the temperature and specific humidity behind the greening layer, which serves as the boundary conditions for the adjacent wall or substrate, we assume that they correspond with the in-canopy values:

$$T_{\mathrm{a}}^{*} = T_{\mathrm{a}}^{\mathrm{C}} \text{ and } q_{\mathrm{a}}^{*} = q_{\mathrm{a}}^{\mathrm{C}}$$

4.4 Calculating the greening canopy leaf temperature

The estimation of the average temperature of the leaves inside the greening layer, including the turbulent fluxes for heat and vapour, is a fundamental step in the simulation of the green facades and roofs.

Like shown for the calculation of the wall surface temperature (see Part 1), the energy budget equation of the leaf needs to be solved for $EB \cong 0$ to find the steady state temperature of the leaf:

$$EB = Q^{L}_{SW,net} + Q^{L}_{LW,net} - H^{L} - LE^{L} \cong 0 \tag{4.47}$$

Here $Q^{L}_{SW,net}$ is the net shortwave radiation absorbed at the leaf surface, $Q^{L}_{LW,net}$ is the longwave radiation budget of the leaf and H^{L} and LE^{L} are the fluxes of sensible and latent heat from/to the leaf surface.

4.4.1 Radiative components $Q^{L}_{\mathrm{SW,net}}$ and $Q^{L}_{\mathrm{LW,net}}$

The shortwave radiation budget of the leaf is composed of the direct and diffuse component in the middle of the greening layer as calculated by (4.9) and (4.19):

$$Q^{L}_{\mathrm{SW,net}} = \tau_{\mathrm{L}} \cdot \Big(Q^{\mathrm{C}}_{\mathrm{SW,dir}} + Q^{\mathrm{C}}_{\mathrm{SW,dif}} \Big) \tag{4.48}$$

where τ_{L} is the absorption coefficient of the leaf for shortwave radiation defined as

$$\tau_{\mathrm{L}} = 1 - \alpha_{\mathrm{L}} - \iota_{L} \tag{4.49}$$

using the leaf albedo α_L and its transmission coefficient ι_L, both defined in the vegetation database.

The longwave budget depends on the incoming longwave radiation in the canopy center Q^C_LW as given by (4.31) and the actual leaf temperature T_L:

$$Q^L_{\mathrm{LW,net}} = Q^\mathrm{C}_\mathrm{LW} - 2\Big((1-\varepsilon_\mathrm{L})\cdot Q^\mathrm{C}_\mathrm{LW} + \sigma_B\cdot\varepsilon_\mathrm{L}\cdot T^4_\mathrm{L}\Big) \quad (4.50)$$

It is important to note that the longwave radiation budget of the leaf has to be calculated bi-directionally, as the leaf receives longwave radiation from both sides (see Fig. 5, p. 8), but also emits to both sides of the leaf.

4.4.2 Turbulent fluxes

The energy fluxes due to the exchange of sensible and latent heat between leaves and atmosphere are given by:

$$\begin{aligned} H^L &= c_p\rho_a\cdot j_H && (4.51)\\ LE^L &= \rho_a L(T_L)\cdot(j_E + j_T) && (4.52)\end{aligned}$$

where j_H is the flux of sensible heat, j_E is the evaporation flux from or to the leaf surface and j_T is the transpiration flux from the leaf stomata into the air.

The latent heat of evaporation L is depending on a reference temperature, in this case the leaf temperature $T = T_L$.

$$L(T) = (2.501 - 0.00237\cdot T)\cdot 1e^6 \quad (4.53)$$

Sensible Heat flux j_H

For a given leaf temperature T_L and a given in-canopy air temperature T^C_a the turbulent flux of sensible heat can be written as:

$$j_H = 1.1\frac{1}{r_a}\big(T_L - T^\mathrm{C}_a\big) \quad (4.54)$$

Following Braden (1982), the aerodynamic resistance r_a at the leaf surface can be calculated as function of the typical leaf geometry (A and D) and the local wind speed u^C:

$$r_a = A\sqrt{\frac{D}{\max(u^\mathrm{C}, 0.05)}} \quad (4.55)$$

with a lower wind speed limit of 0.05 ms^{-1}.

For deciduous leaves and grass-like plants, the parameter A is set to 87 $\sqrt{\mathrm{s}}\mathrm{m}^{-1}$, but for dense vegetation like mosses, it may approach up to 200 $\sqrt{\mathrm{s}}\mathrm{m}^{-1}$. The variable D represents the typical leaf diameter and is set to 0.02 m for herbaceous plants and 0.15 m for deciduous plants.

It's worth noting that these values are based on regular trees and vegetation and not wall or roof plants. Therefore, adjustments may be necessary, although the impact of this single parameter is minimal.

Vapour flux j_E and j_T

The vapour flux between the leaf and the atmosphere is composed of two components: The evaporation term j_E and the transpiration term j_T.

While the evaporation term depends solely on the vapour saturation deficit between the leaf and the surrounding air, the transpiration term represents complex plant physiological processes associated with photosynthesis and water management.

By utilising the resistance factors concept, as seen in the calculation of sensible heat flux, we can define the **evaporation flux** from the leaf as:

$$j_E = \frac{1}{r_a}\cdot\begin{cases} f_w\Delta q & \text{; if } \Delta q \geq 0 \text{ (Evaporation)}\\ \Delta q & \text{; if } \Delta q < 0 \text{ (Condensation)}\end{cases} \quad (4.56)$$

with the aerodynamic resistance r_a as defined in (4.55).

The saturation deficit at a given leaf temperature T_L can be written as

$$\Delta q = q_*(T_L) - q^\mathrm{C}_a \quad (4.57)$$

where q_* is the specific air humidity at saturation value.

The parameter f_w denotes the proportion of the leaf area that is wet at the simulated time and therefore is capable of water evaporation. Its estimation is based on Deardorff (1978)'s method.

$$f_w = \left(\frac{W_\mathrm{dew}}{W_\mathrm{dew,max}}\right)^{2/3} \quad (4.58)$$

where W_dew is the amount of liquid water on the leaf surface and W_dew is its maximum value set to

$$W_\mathrm{dew,max} \approx LAD_C\Delta_C\cdot 0.2\mathrm{kgm}^{-2} \quad (4.59)$$

The quantity of water on the leaf (W_dew) is calculated by the main plant model as a prognostic variable, which is updated for each time step of the simulation, considering evaporation, transpiration or rain fall.

In addition to this, for the transpiration flux, the vegetation incorporates an extra physiological control variable, which takes into account the plant stomata's behaviour by means of stomata resistance (r_s).

$$\dot{j}_T = \frac{1}{r_a + r_s} \cdot \begin{cases} (1 - f_w)\Delta q & ;\text{if } \Delta q \geq 0 \text{ (Transpiration)} \\ 0 & ;\text{if } \Delta q < 0 \end{cases} \tag{4.60}$$

Transpiration occurs only when the air within the canopy is undersaturated. The ENVI-met vegetation module MiPSS provides the calculation for stomata resistance r_s, which is comprehensively described in a separate technical report.

The required input parameters are taken from the different microclimate variables discussed in the sections above. Additionally, the stomata model receives the water availability coefficient (ζ_w), which is set to ζ_w=1 for plants without substrate or as a user-adjustable parameter ζ_w=[0..1] for GWS with a substrate layer.

5 Modelling the Substrate Layer

The current description of the green wall system depicts it solely as a vegetation layer, without any possibility for localized growth of plants on the facade or roof. Typical applications are climbing plants rooting at the ground surface or plants hanging from the roof.

This section introduces an extension to the greening model with a substrate layer, facilitating the simulation of green systems where plants can be grown locally on the façade or roof, e.g. living wall systems.

5.1 General model concept

Figure 7 presents the green wall model, which incorporates a substrate layer. Similar to the building wall model, the substrate component is divided into three individual layers, encompassing a total of 7 calculation nodes for the temperature distribution calculation. This detailed subdivision takes into account that the substrate of a vegetation system usually consists not only of the substrate itself, but also of a fixing material and possibly an outer canvas to protect the substrate. Consequently, the phrase "*substrate*" encompasses any technical materials employed in the construction of the green wall system.

Air gap to the building wall

One important detail with respect to the construction of the greening system with substrate is its attachment to the building wall. Here, the model design supports two possible scenarios:

- The substrate layer is directly attached to the wall or roof (Air gap Δ_{AG}=0),
- An air gap of size Δ_{AG} is present between the substrate/plant system and the building wall

The second option is more frequently used, but we will start the description with the first option, no air gap, as the latter is the more complex extension of the model.

Substrate Temperature and Water

As previously discussed, it is assumed that green wall systems require a managed water supply, or else they will likely perish. Hence, the water balance of the substrate is not a prognostic factor of the greening model and does not affect either transpiration from the plants or direct evaporation from the substrate. Rather than calculating a water balance, the model uses a user-defined *Watering Coefficient* (WC), which ranges between 0 (dry) and 1 (fully saturated). Details will be covered in later sections.

Consequently, the prognostic equations for the condition of the substrate layer are limited to the description of the heat transfer between the calculation points, taking into

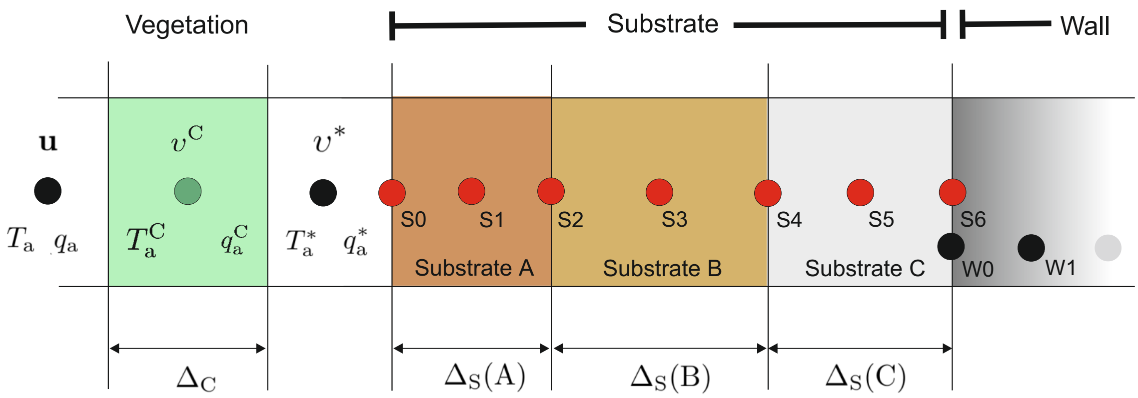

Figure 7: Concept diagram of a green wall system with greening layer plus substrate layer including the main prognostic variable

account the physical properties of the natural or artificial material inside the construction.

5.2 Temperature distribution inside the substrate layer

As shown in Figure 7, the substrate is discretized into three individual material layers A, B and C of thickness $\Delta_S(A)$, $\Delta_S(B)$ and $\Delta_S(C)$. Like in the wall model (compare Part 1), each layer has a prognostic calculation point in its center and two on the lateral borders resulting in seven points in total.

The temperature distribution inside the substrate system is given by the one-dimensional Fourier Equation:

$$\frac{\partial T_i}{\partial t} = \kappa_S(i) \frac{\partial^2 T_i}{\partial \Delta_{S,i}^2} \tag{5.1}$$

where $\kappa_S(i)$ is the relevant thermal diffusivity of the substrate or other material at node i in $[\mathrm{m}^2\mathrm{s}^{-1}]$ and $\Delta_{S,i}$ is the distance between the calculation nodes.

Many aspects of this equation, including the method of solution, are similar to the heat transfer equation in the building wall, so we will restrict ourselves here to those aspects that are unique to the substrate system.

5.2.1 Defining the substrate or material thermal properties

In order to solve the Fourier equation for heat transfer, it is essential that the thermal conductivity and heat capacity of the substrate are known. It is important to note that, in contrast to simulating a building wall or roof, the thermal behavior of the substrate cannot merely be assumed as a constant property of the material. If the substrate is capable of retaining liquid water -which should be the case for at least one layer of the substrate system - the thermal properties of the substrate will depend on the distribution of water and air within the material.

The thermal conductivity κ_S of the substrate can be written as the quotient of the thermal conductivity of the material λ_S and the volumetric heat capacity $\rho_S c_S$:

$$\kappa_S = \frac{\lambda_S}{\rho_S c_S} \tag{5.2}$$

For a porous material, both components depend on the amount of liquid water inside the layer. The actual volumetric heat capacity $\rho_S c_S$ is weighted between the heat capacity of the material itself $\rho_i c_i$ and the heat capacity of water $\rho_w c_w$:

$$\rho_S c_S = (1 - \eta_s)\, \rho_i c_i + \eta \cdot \rho_w c_w \tag{5.3}$$

where η is the actual water content of the substrate (see below) and η_s is its maximum value at saturation point.

The thermal conductivity of the substrate-water-air mixture λ_S can be obtained using the actual matrix potential of the substrate Ψ^{cm} in cm (=100Ψ_i) after Tjernström (1989):

$$\lambda_S = \begin{cases} 419 \exp - \left[(\log |\Psi_i^{\mathrm{cm}}| + 2.7) \right] & ; \text{if } \log |\Psi_i^{\mathrm{cm}}| \leq 5.1 \\ 0.172 & ; \text{if } \log |\Psi_i^{\mathrm{cm}}| > 5.1 \end{cases} \tag{5.4}$$

The actual matrix potential of the substrate can be obtained from the substrate water content η, its value at saturation point η_s and the empirical Clapp and Hornberger constant b:

Table 1: Hydraulic and thermodynamic parameter of different natural soils/ substrates and artificial materials after Clapp and Hornberger (1978); Kuchling (1991)

Water content at η_s: Saturation value, η_{fc}: Field capacity, η_{wilt}: Wilting point; Ψ_s: Matrix potential at saturation value, $K_{\eta,s}$: Hydraulic conductivity, b: *Clapp and Hornberger constant*, $\rho_i c_i$: Volumetric heat capacity of material (without water), λ : Thermal conductivity of material (if constant)

	η_s	η_{fc}	η_{wilt}	Ψ_s	$K_{\eta,\mathrm{s}}$	b	$\rho_i c_i$	λ
Soils and Substrates								
Sand	0.385	0.135	0.0068	-0.121	176.0	4.05	1.463	
Loamy Sand	0.410	0.150	0.075	-0.090	156.3	4.38	1.404	
Sandy Loam	0.435	0.195	0.114	-0.218	34.1	4.90	1.320	
Silt Loam	0.485	0.255	0.179	-0.786	7.2	5.30	1.271	
Loam	0.451	0.240	0.155	-0.478	7.0	5.39	1.212	
Sandy Clay Loam	0.420	0.255	0.175	-0.299	6.3	7.12	1.175	
Silty Clay Loam	0.477	0.322	0.218	-0.356	1.7	7.75	1.317	
Clay Loam	0.476	0.325	0.250	-0.630	2.5	8.52	1.225	
Sandy Clay	0.426	0.310	0.219	-0.153	2.2	10.40	1.175	
Silty Clay	0.492	0.370	0.283	-0.490	1.0	10.40	1.150	
Clay	0.482	0.367	0.286	-0.405	1.3	11.40	1.089	
Peat	0.863		0.395	-0.356	8.0	7.75	0.836	
Construction Materials								
Styrofoam							0.200	0.10
Smashed Brick							2.000	1.00
Granite							2.345	4.61
Basalt							2.386	1.73

Units: $[\eta_s]$, $[\eta_{\mathrm{fc}}]$, $[\eta_{\mathrm{wilt}}] = \mathrm{m^3 m^{-3}}$,$[\Psi_s] = \mathrm{m}$, $[K_{\eta,\mathrm{s}}] = 10^{-6}\mathrm{ms^{-1}}$, $[\rho_i c_i] = 10^6\mathrm{Jm^{-3}K^{-1}}$, $[\lambda] = \mathrm{Wm^{-1}K^{-1}}$

$$\Psi = \Psi_s \left(\frac{\eta_s}{\eta}\right)^b \tag{5.5}$$

As mentioned above, the water content of the substrate is not a prognostic variable in the GWS model, but is kept constant by the watering factor ζ_w with a range of 0 to 1, which can be defined by the user. This factor is defined, as in the main ENVI-met soil model, as the fraction of the usable field capacity, so that the actual water content η of the substrate can be determined using η_w, the field capacity η_{fc} and the wilting point η_{wilt} of the substrate:

$$\eta = \zeta_w \cdot (\eta_{\mathrm{fc}} - \eta_{\mathrm{wilt}}) + \eta_{\mathrm{wilt}} \tag{5.6}$$

Table 1 displays a collection of natural soils and substrates alongside construction materials, including their hydraulic properties and Clapp and Hornberger constant b, utilized in the ENVI-met soil model.

It is essential to note that the initial study by Clapp and Hornberger (1978) concentrated on natural soils, whereas modern materials and substrates could possess varying hydraulic properties. As the relevant data is stored in the database, users can supplement it with additional information that pertains to specific materials.

5.2.2 Boundary conditions I: Substrate outer surface

As with building walls, an extra energy balance equation must be solved to determine the outer surface temperature $T_{\mathrm{S},0}$ of the substrate system. Since the substrate cannot function without greening, the modified radiative fluxes and adjusted microclimate variables, as discussed in Sections 4.2 and 4.3 for the building wall, now serve as input parameters for the substrate layer.

$$Q^{\mathrm{S}}_{\mathrm{SW,net}} + Q^{\mathrm{S}}_{\mathrm{LW,net}} - H^{\mathrm{S}} - LE^{\mathrm{S}} - G^{\mathrm{S}} = 0 \tag{5.7}$$

Radiative Fluxes

The radiative fluxes are solved analogously to the building wall with

$$Q^{\mathrm{S}}_{\mathrm{SW,net}} = \tau_{\mathrm{S}} \cdot \Big(\cos(\beta) \cdot Q^*_{\mathrm{SW,dir}} + Q^*_{\mathrm{SW,dif}}\Big) \tag{5.8}$$

for the shortwave net radiation and

$$Q^{\mathrm{S}}_{\mathrm{LW,net}} = Q^*_{\mathrm{LW}} - \Big((1-\varepsilon_{\mathrm{S}}) \cdot Q^*_{\mathrm{LW}} + \sigma_B \cdot \varepsilon_{\mathrm{S}} \cdot T^4_{\mathrm{S},0}\Big) \tag{5.9}$$

for the longwave counterpart. The modified components of the radiation behind the greening layer

($Q^*_{\mathrm{SW,dir}}$,$Q^*_{\mathrm{SW,dif}}$ and Q^*_{LW}) are now used as input for the radiative balance. For the shortwave absorption τ_{S} and the longwave emissivity ε_{S} the properties of the outermost substrate layer are used.

Turbulent Fluxes

The turbulent flux of **sensible heat** H^{S} between the substrate and the air is given by

$$H^{\mathrm{S}} = h_c^{\mathrm{S}} \cdot (T_{\mathrm{S},0} - T_{\mathrm{a}}^{\mathrm{C}}) \tag{5.10}$$

using the in-canopy air temperature $T_{\mathrm{a}}^{\mathrm{C}}$ as microclimate reference and calculating the heat transfer coefficient h_c^{S} like for the building wall (compare Section 2.2.2 in Part 1 of this paper), but using the modified wind speed v^* behind the greening layer as reference wind speed.

The turbulent flux of latent heat LE^{S} is only considered if the outermost substrate layer contains a material that can hold and evaporate liquid water. In this case the flux can be written as

$$LE^{\mathrm{S}} = L(T_{\mathrm{S},0}) \cdot \frac{h_c}{c_p} \cdot \left(q_{\mathrm{S},0} - q_{\mathrm{a}}^{\mathrm{C}}\right) \tag{5.11}$$

To calculate LE, the specific humidity directly at the substrate surface $q_{\mathrm{S},0}$ must be known, which depends on the substrate temperature, the humidity of the surrounding air and water availability of the substrate.

According to Deardorff or Mihailović and Rajković (Deardorff, 1978; Mihailović and Rajković, 1994), the surface humidity can be accurately determined using the beta approach, which involves calculating the appropriate weighting between the surface humidity at saturation $q^{\mathrm{sat}}(T_{\mathrm{S},0})$ and the specific humidity behind the greening layer q_a^*:

$$q_{\mathrm{S},0} = \beta q^{\mathrm{sat}}(T_{\mathrm{S},0}) + (1-\beta) q_a^* \tag{5.12}$$

The β factor relates the actual humidity of the outer substrate layer η to its value at field capacity η_{fc} (see Tab. 1):

$$\beta = \min\left(1, \frac{\eta}{\eta_{\mathrm{fc}}}\right) \tag{5.13}$$

Finally, the **conductive heat transfer** G^{S} between the surface and next calculation node in the substrate system $T_{\mathrm{S},1}$ needs to be defined. Here, the formulation is similar to the heat transfer in the building wall with

$$G^{\mathrm{S}} = \frac{\lambda_{\mathrm{S,A}})}{0.5 \cdot \Delta_{\mathrm{S}}(\mathrm{A}) \cdot (T_{\mathrm{S},0} - T_{\mathrm{S},1})} \tag{5.14}$$

with the thermal conductivity of substrate material A $\lambda_{\mathrm{S,A}}$ calculated after eq. 5.4.

5.2.3 Boundary conditions II: Substrate inner surface

Additional boundary conditions are required for the side of the substrate facing the building wall. Currently, we assume that there is no air gap between the substrate and the building wall. Thus, as demonstrated in Figure 7, we consider the inner node of the substrate $T_{\mathrm{S},6}$ and the outer node of the building wall $T_{\mathrm{W},0}$ to be identical.

$$T_{\mathrm{S},6} = T_{\mathrm{W},0}$$

In this case there is no need to solve an additional energy balance for the inner node of the substrate layer, nor is there a need to solve the energy balance for the outer building wall node $T_{\mathrm{W},0}$. Both thermal systems are connected, and the temperature at all internal points is determined by the change in the outer substrate temperature, $T_{\mathrm{S},0}$, and the temperature dynamics of the inner building wall surface, $T_{\mathrm{W},6}$. This is elaborated in Part I of this paper.

5.2.4 Outgoing fluxes from the substrate

The substrate layer covering the building wall or roof replaces the radiative and turbulent fluxes originating from the building. Section 3.2, p. 3, eqs. (3.7) and (3.8) define the outgoing shortwave and longwave radiation from the building wall. With the presence of a substrate layer, these fluxes are replaced for the shortwave component by:

$$Q_{\mathrm{SW,out}} = \alpha_{\mathrm{S}} \cdot \left(Q^*_{\mathrm{SW,dir}} + Q^*_{\mathrm{SW,dif}}\right) \tag{5.15}$$

and for the longwave radiation with

$$Q_{\mathrm{LW,out}} = (1-\varepsilon_{\mathrm{S}}) \cdot Q^*_{\mathrm{LW}} + \sigma_B \cdot \varepsilon_{\mathrm{S}} \cdot T^4_{\mathrm{S},0} \tag{5.16}$$

If the outermost substrate layer can exchange humidity with the air, and **additional vapour flux** j_{S} needs to be considered when calculating the humidity inside the greening layer.

Here, we can write

$$j_{\mathrm{S}} = \frac{h_c}{c_p \rho_a} \cdot \left(q_{\mathrm{S},0} - q_{\mathrm{a}}^*\right) \tag{5.17}$$

As for the walls of the building, Section 6 discusses the interaction of the outgoing turbulent fluxes of sensible heat and vapour with the atmosphere.

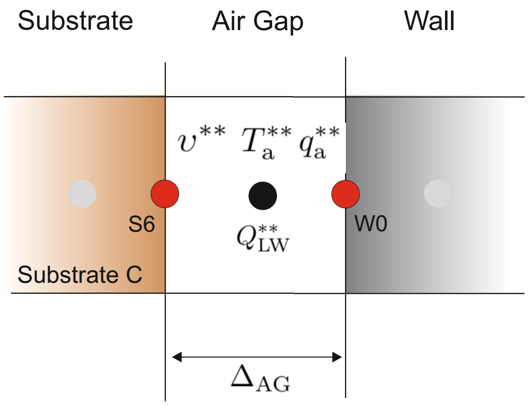

Figure 8: Concept diagram of a green wall system with air gap including the main prognostic variables

5.3 Modelling an additional air gap

As a concluding aspect of the green wall model design, the presence of an air gap between the substrate layer and the building wall needs to be taken into account. The width of the air gap, defined as Δ_{AG}, must not be below 0.05 m to maintain numerical stability, otherwise the air gap is removed.

5.3.1 Microclimate conditions in the air gap

Inside the air gap, a very low air circulation is assumed:

$$\upsilon^{**} = 0.1$$

As the corresponding substrate his opaque, all **shortwave radiation** values inside the air gap are set to 0:

$$Q_{\mathrm{SW,dir}}^{**} = Q_{\mathrm{SW,dif}}^{**} = Q_{\mathrm{SW,refl}}^{**} = 0$$

The **longwave radiation** in the air gap Q_{LW}^{**} is affected from both the emitted longwave radiation from inner substrate layer $Q_{\mathrm{LW,S*}}$ and from the building wall $Q_{\mathrm{LW,W*}}$:

$$Q_{\mathrm{LW}}^{**} = 0.5 \cdot Q_{\mathrm{LW,S*}} + 0.5 \cdot Q_{\mathrm{LW,W*}} \tag{5.18}$$

with

$$\begin{aligned} Q_{\mathrm{LW,S*}} =& (1-\varepsilon_{\mathrm{S}}) \cdot \sigma \cdot T_{\mathrm{W,0}}^4 + \varepsilon_{\mathrm{S}} \cdot \sigma \cdot T_{\mathrm{S,6}}^4 \\ Q_{\mathrm{LW,W*}} =& (1-\varepsilon_{\mathrm{W}}) \cdot \sigma \cdot T_{\mathrm{S,6}}^4 + \varepsilon_{\mathrm{W}} \cdot \sigma \cdot T_{\mathrm{W,0}}^4 \end{aligned}$$

To determine the **air temperature** in the air gap (T_{a}^{**}), a mixing approach similar to the in-canopy air is used:

$$T_{\mathrm{a}}^{**} = T_{\mathrm{a}}^{*} + 0.5 \cdot \left(\Delta T_{\mathrm{S*}} + \Delta T_{\mathrm{W*}}\right)\Delta t \tag{5.19}$$

This approach assumes that the air temperature in the air gap is affected by the simulated air temperature behind the substrate (see section 4.3.4, p. 10) and by the temperature fluxes from both the inner substrate layer and the wall.

The temperature flux from the substrate $\Delta T_{\mathrm{S*}}$ can be determined by.

$$\Delta T_{\mathrm{S*}} = A^{**} \cdot \frac{h_c}{c_p \rho_a} \cdot \left(T_{\mathrm{S,6}} - T_{\mathrm{a}}^{*}\right) \tag{5.20}$$

and the flux from the building wall $\Delta T_{\mathrm{W*}}$ is defined as

$$\Delta T_{\mathrm{W*}} = A^{**} \cdot \frac{h_c}{c_p \rho_a} \cdot \left(T_{\mathrm{W,0}} - T_{\mathrm{a}}^{*}\right) \tag{5.21}$$

with h_c calculated for the air flow inside the gap υ^{**} set to 0.1 m/s.

The scaling factor A^{**} now relates the wall and substrate surface area to the volume of the air gap:

$$A^{**} = \frac{A}{A \cdot \Delta_{\mathrm{AG}}} \text{ with } A = \begin{cases} \Delta y \Delta z \text{ ;X-Walls} \\ \Delta x \Delta z \text{ ;Y-Walls} \\ \Delta x \Delta y \text{ ;Roofs/ Z-Walls} \end{cases} \tag{5.22}$$

For the **specific humidity** in air gap we use a similar approach like for the air temperature, but in this case only the substrate layer can influence the specific humidity inside the gap:

$$q_{\mathrm{a}}^{**} = q_{\mathrm{a}}^{*} + \Delta q_{\mathrm{S*}} \cdot \Delta t \tag{5.23}$$

with the humidity flux from the substrate layer given as

$$\Delta q_{\mathrm{S*}} = A^{*} \cdot \frac{h_c}{c_p \rho_a} \cdot \left(q_{\mathrm{S,6}} - q_{\mathrm{a}}^{*}\right) \tag{5.24}$$

The surface humidity of the inner substrate layer $q_{\mathrm{S,6}}$ is calculated analogously to eq. 5.12, but using the water content of the inner substrate layer as reference humidity η.

5.3.2 Modified boundary conditions for the wall and substrate inner surface

The presence of the air gap modifies the boundary conditions for both the adjacent building wall and the inner surface of the substrate.

Previously we have assumed a direct connection between the substrate and the wall, so no handling of the energy balance of the wall and of the inner substrate layer was required. With the introduction of an additional air gap, both the energy balance for the building wall needs to be solved plus an additional energy balance for the inner side of the substrate system to obtain the substrate temperature $T_{\mathrm{S},6}$.

Detailed discussions on both procedures can be found in Section 3 (p. 3) for the wall under non-greened conditions or in Section 5.2.2 (p. 14) for the outer side of the substrate.

The solution for the building wall under modified conditions and for the inner substrate is analogous to the methods presented in these paragraphs and will not be discussed further. Only the relevant input variables in the calculation procedures need to be replaced by their updated values valid inside the air gap.

6 Coupling with the main ENVI-met model

The modified microclimate conditions at a green wall or roof do not only influence the energy balance of the underlying building wall, but also interact with the main ENVI-met model. These interactions affect the radiative fluxes on one hand and the turbulent fluxes of heat and vapour on the other.

6.1 Modified radiative fluxes

The complex interactions between the GWS and the shortwave and longwave radiation fluxes have been discussed in detail in Section 4.2.1, p. 5 for the shortwave and in Section 4.2.3, p. 7 for the longwave fluxes.

For the interaction with the main ENVI-met model, the outgoing fluxes $Q^{\mathrm{G,sum}}_{\mathrm{SW,dif}}$ for the reflected shortwave radiation at the GWS and $Q^{\mathrm{G}}_{\mathrm{LW}}$ for the outgoing longwave radiation are relevant for the microclimate simulation.

The updated fluxes are used to calculate the received radiation at other elements in the model, such as buildings, ground surfaces or vegetation. The IVS technique ascertains the most precise consideration of these effects by calculating individual view factors for all model elements. For further information regarding the IVS method and calculation of view factors, please refer to Simon et al. (2021).

6.2 Modified turbulent fluxes

Sensible Heat Flux

The prognostic equation for the potential air temperature θ in ENVI-met is given by the three-dimensional combine advection-diffusion equation

$$\begin{aligned}\frac{\partial\theta}{\partial t}+u\frac{\partial\theta}{\partial x}+v\frac{\partial\theta}{\partial y}+w\frac{\partial\theta}{\partial z} &= \\ &\frac{\partial}{\partial x}\left(K_h\frac{\partial\theta}{\partial x}\right)+\frac{\partial}{\partial y}\left(K_h\frac{\partial\theta}{\partial y}\right)+\frac{\partial}{\partial z}\left(K_h\frac{\partial\theta}{\partial z}\right) \\ &+\frac{1}{c_p\rho}\nabla Q_{\mathrm{lw}}(x,y,z)+S_\theta(x,y,z)\end{aligned} \tag{6.1}$$

where ∇Q_{lw} is the change of air temperature due to divergences in the longwave radiation fluxes and S_θ is an universal source/sink term that sums up all changes of air temperature due to fluxes of sensible heat in the model. K_h is the atmospheric exchange coefficient for heat provided by the ENVI-met turbulence model.

To incorporate the fluxes at the building walls, we define a source/sink component with

$$S_\theta^W = K_h^* \frac{T_{\mathrm{W,Mix}} - T_\mathrm{a}}{(\Delta_\mathrm{W})^2} \tag{6.2}$$

In this context, $T_{\mathrm{W,Mix}}$ represents the theoretical temperature of the wall, which considers the structure of the green wall system and the density of the vegetation. [1]

If a wall lacks a substrate layer, the mixed wall temperature, $T_{\mathrm{W,Mix}}$, is determined by combining the leaf temperature, T_L, and the underlying building wall temperature, $T_{\mathrm{W},0}$, in proportion to the greening factor ω_G as defined in (4.34).

$$T_{\mathrm{W,Mix}} = \omega_\mathrm{G} \cdot T_\mathrm{L} + (1 - \omega_\mathrm{G}) \cdot T_{\mathrm{W},0} \tag{6.3}$$

If a substrate layer is present, the wall facade temperature is replaced by the surface temperature of the outer substrate layer $T_{\mathrm{S},0}$:

$$T_{\mathrm{W,Mix}} = \omega_\mathrm{G} \cdot T_\mathrm{L} + (1 - \omega_\mathrm{G}) \cdot T_{\mathrm{S},0} \tag{6.4}$$

For the exchange coefficient for heat K_h^* between the GWS and the atmosphere, a similar concept of is applied. We define the turbulent exchange coefficients at the building wall, at the leafs and (if present) at the substrate layer. For the bare wall the exchange coefficient can be calculated as :

$$K_h^\mathrm{W} = \frac{h_c^\mathrm{W} \cdot \Delta_\mathrm{W}}{c_p \rho_a} \tag{6.5}$$

using the heat transfer coefficient h_c^W as given in eq. 3.4, p. 3. For the leaves of the greening layer, the formulation can be written as

$$K_h^\mathrm{L} = \frac{1}{r_a} \cdot \Delta_\mathrm{W} \tag{6.6}$$

using the aerodynamic resistance of the the leafs given by eq. 4.55, p. 11.

For the exchange coefficient at the substrate layer, we get

$$K_h^\mathrm{S} = \frac{h_c^\mathrm{S} \cdot \Delta_\mathrm{W}}{c_p \rho_a} \tag{6.7}$$

using the heat transfer coefficient h_c^S analogously to eq. 5.10, p. 15.

Finally, the overall exchange coefficient for a GWS without substrate layer can be written as:

$$K_h^* = \omega_\mathrm{G} \cdot K_h^\mathrm{L} + (1 - \omega_\mathrm{G}) \cdot K_h^\mathrm{W} \tag{6.8}$$

If a substrate layer is present, the exchange at the building wall is replaced by the transfer at the outer substrate layer:

$$K_h^* = \omega_\mathrm{G} \cdot K_h^\mathrm{L} + (1 - \omega_\mathrm{G}) \cdot K_h^\mathrm{S} \tag{6.9}$$

Vapur Flux

The prognostic equation for the specific humidity of the air is given by:

$$\begin{aligned}\frac{\partial q}{\partial t} + u\frac{\partial q}{\partial x} + v\frac{\partial q}{\partial y} + w\frac{\partial q}{\partial z} = \\ \frac{\partial}{\partial x}\left(K_h \frac{\partial q}{\partial x}\right) + \frac{\partial}{\partial y}\left(K_h \frac{\partial q}{\partial y}\right) + \frac{\partial}{\partial z}\left(K_h \frac{\partial q}{\partial z}\right) \\ + S_q(x,y,z)\end{aligned} \tag{6.10}$$

Analogously to the concept of the temperature equation, the source/sink term S_q is used to include effects that lead to a sink or source of humidity into the prognostic equation.

For the GWS, the source/ sink term for grid points directly connected to a green wall can written as:

$$S_q = (j_\mathrm{E} + j_\mathrm{T}) \cdot LAD^* + j_\mathrm{S} \cdot A^* \tag{6.11}$$

where j_E is the evaporation flux of the greening layer given by eq. 4.56 and j_T is the transpiration flux of the leaves after eq. 4.60. Both fluxes are scaled with LAD^* as given by eq. 4.42.

If a substrate layer is present, the humidity flux from the outer layer j_S (see eq. 5.17, scaled with A^* after eq. 4.46) also contributes to the vapour exchange with the atmosphere and is added to the source/ sink term.

1. If the atmospheric pressure in the model differs from the standard pressure of 1013 hPa, potential air temperature θ and absolute temperature T must be adapted accordingly before using them in conjunction.

7 Example Study

A small case study is presented to show the performance of different greening configurations using ENVI-met V5.5 and to explain the structure of output variables.

The case study model area has a size of $90\times50\times25$ cells in $2\,\mathrm{m}$ resolution and contains seven buildings, with a size of $20\times20\times10\,\mathrm{m}$ each (Fig. 9):

1. Default Building without any greening
2. Building with only greening (DB item copy of `02NAFG` with low LAI of 0.75)
3. Building with only greening (DB item `02NAFG` with high LAI of 1.5)
4. Building with greening and substrate but no air gap (DB item copy of `02NGSS` with low LAI of 0.75)
5. Building with greening and substrate but no air gap (DB item `02NGSS` with high LAI of 1.5)
6. Building with greening and substrate with air gap (DB item copy of `02AGSS` with low LAI of 0.75)
7. Building with greening and substrate with air gap (DB item `02AGSS` with high LAI of 1.5)

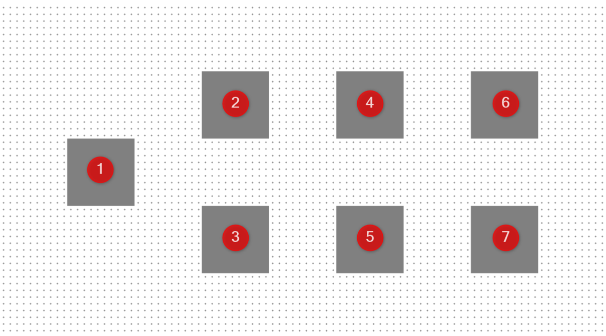

Figure 9: Model area design for the case study

Climate Conditions

This study simulates a typical summer day in Central Europe, specifically in Mainz, Germany.

The model utilizes a Full Forcing derived from an EPW file of Frankfurt am Main, a nearby city, to determine radiation, air temperature, and air humidity values. **Radiation data** indicate clear-sky conditions. During the morning hours, the **air temperature** ranges from $17\,°\mathrm{C}$ and rises up to $31\,°\mathrm{C}$ during the afternoon hours. The specific humidity values vary between 10 and $12\,\mathrm{g\,kg^{-1}}$. The Full Forcing does not specify wind conditions, but instead maintains a summer low-wind scenario of $1\,\mathrm{m\,s^{-1}}$ with a direction of 270°.

Model Results

Upon analysis, it is expected that the greatest impact of wall /roof greening can be observed on the bare facade located behind the greening. Specifically, the surface temperature of the wall /roof is stored in the variable '*Wall: Temperature Node 1 outside*'. Whilst the building lacking greenery displays rooftop surface temperatures exceeding $55\,°\mathrm{C}$ during the hot afternoon (15:00), the greened roofs yield much lower rooftop surface temperatures of $38\,°\mathrm{C}$ down to $20\,°\mathrm{C}$ depending on the type of greenery (Fig. 10).

As buildings 4 and 5 do not contain air gaps, they exhibit the coolest temperatures as the roof surface temperature can only be influenced by conduction. The buildings with only greenery applied, i.e. 2 and 3, have the lowest cooling rates due to the lack of shade provided by the substrate. On the other hand, buildings 3, 5, and 7 in the lower rows, having higher LAI values for their greenery, demonstrate a stronger cooling effect compared to their counterparts, buildings 2, 4, and 6, with lower LAI values.

Due to evapotranspiration and shading, greenery typically cools the surrounding air temperature (Manso et al., 2021) near a wall. To investigate this effect, scenario comparisons are often conducted between scenarios with greenery and those with little or no greenery. Therefore, we conducted simulations of the same model area without incorporating greenery onto the buildings.

Comparison maps are utilised to display the cooling effects of the greenery, demonstrated by analysing the potential air temperature through a horizontal cut of the model area at a height of $1.4\,\mathrm{m}$ (refer to Fig. 11).

It has been observed that the cooling effect is stronger in high-LAI greened buildings (approximately $0.8\,\mathrm{K}$) during afternoon hours compared to low-LAI greened buildings (approximately $0.4\,\mathrm{K}$) in this particular scenario. The cool air from buildings upwind is transported downwind due to the westerly wind, resulting in a minor cooling effect at the outflow boundary in the East.

However, comparing air temperatures in front of facades in 3D is not possible with the variable '*Wall: Air temperature in front of wall*' as it only represents the value directly in front of the wall or roof. These values may also include air temperatures within the greening canopy or air gap between the wall/roof and the substrate.

The analysis potential of specific output variables '*Wall:*', '*Greening:*', and '*Substrate:*' is limited to the other GWS in the model area with the same greening and substrate configuration. General comparisons between all facades or comparisons to a non-greened scenario would not be possible due to the lack of data for cells without greening. As a result, these variables are not initially included in the building outputs if there is no greening applied anywhere in the model area.

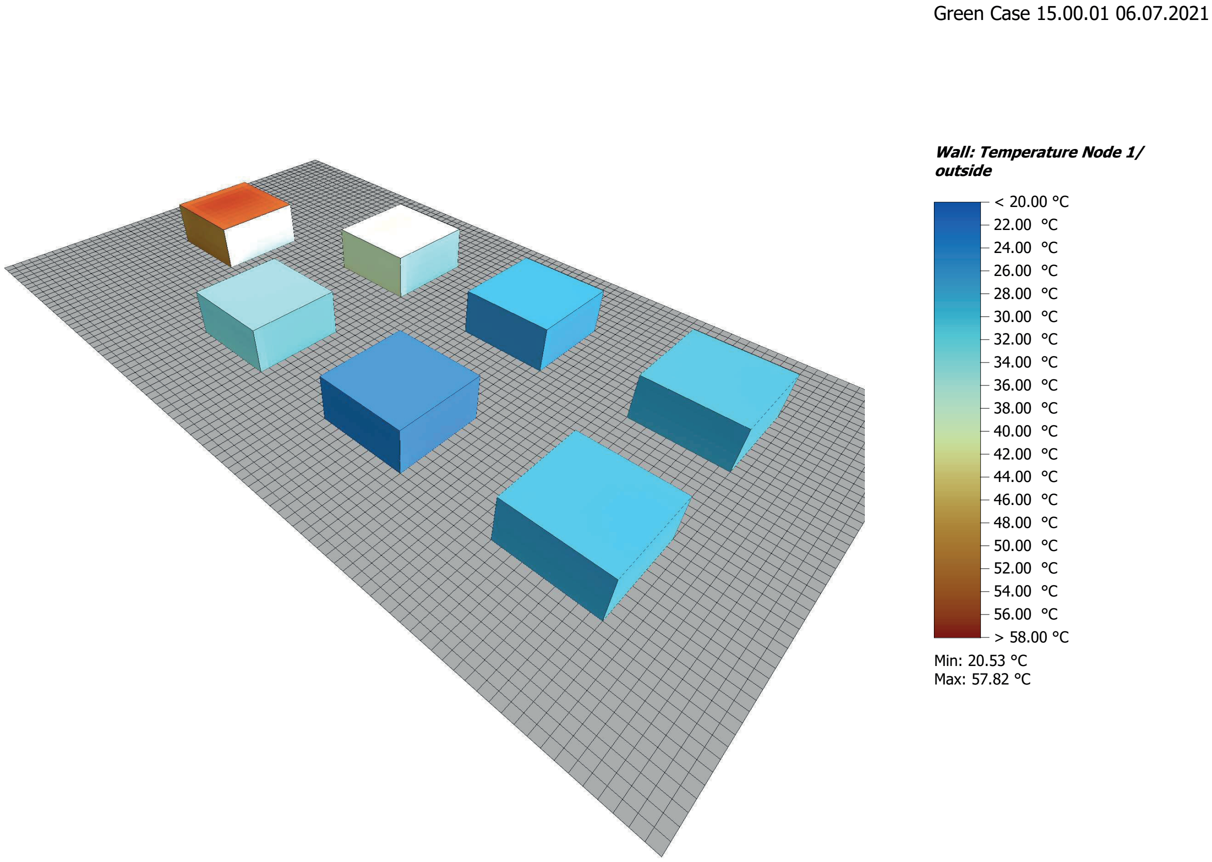

Figure 10: Facade surface temperatures at 15h

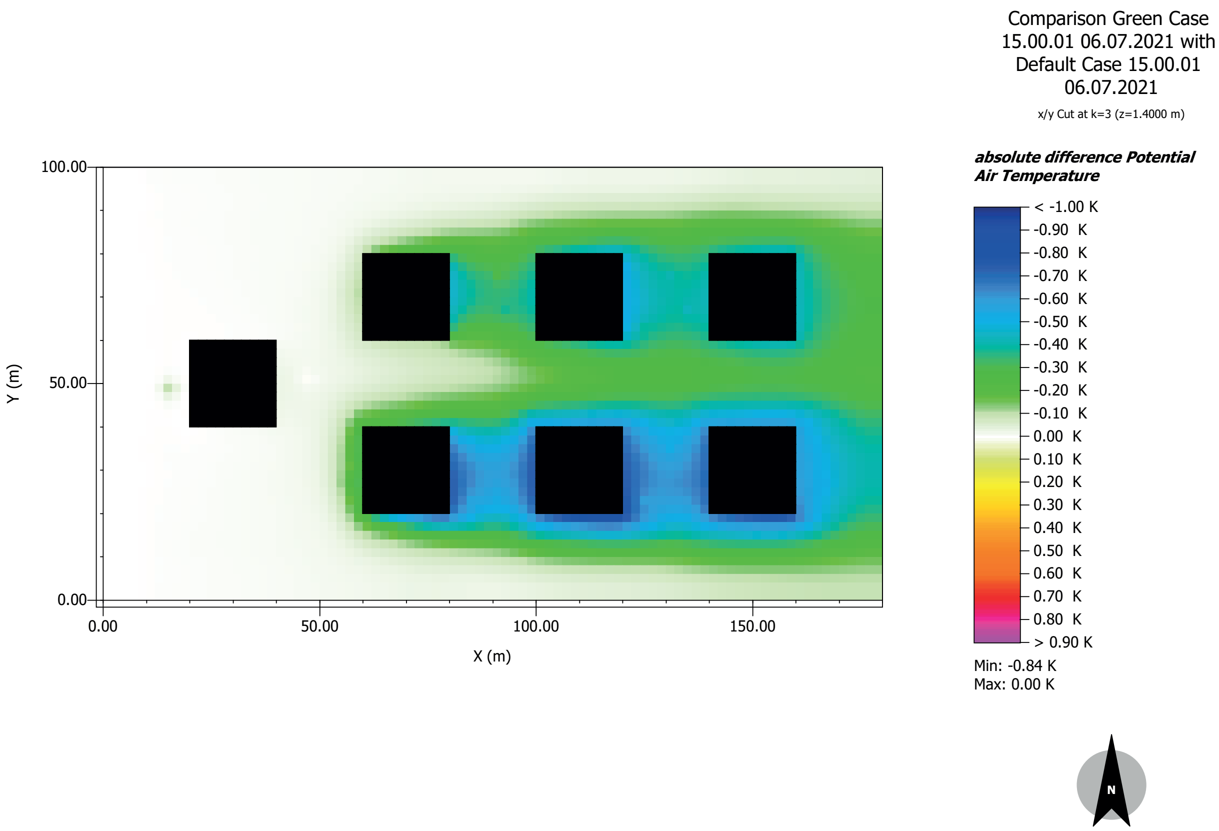

Figure 11: Comparison of air temperatures in $1.4\,\mathrm{m}$ height between greened and non-greened scenario at 15h

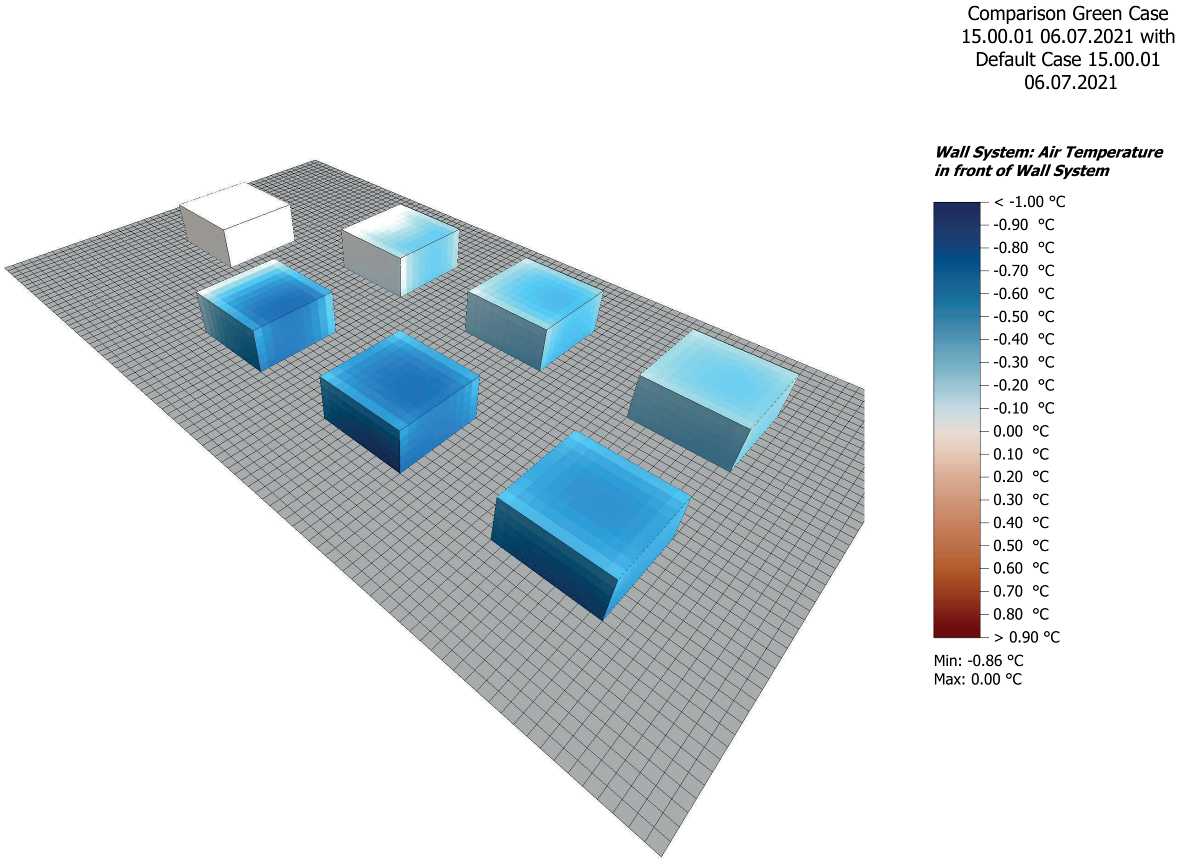

Figure 12: Comparison of air temperatures in front of wall system between greened and non-greened scenario at 15h

To address this problem and ensure consistent comparison of exterior facade states, we have included the '*Wall System*' collection in the building outputs.

In the example '*Air temperature in front of wall*' from above, the '*Wall System:*' collection holds values from directly in front of the wall /roof (if no greening is applied) or in front of the greening (if greening is applied). The figure enables a three-dimensional visualisation of the cooling effect of greenery, by comparing the air temperatures in front of the entire wall system under the greened and non-greened scenarios (see Fig. 12).

References

Balick, L. K., Scoggins, R. K., and Link, L. E. (1981). Inclusion of a Simple Vegetation Layer in Terrain Temperature Models for Thermal IR Signature Prediction. *IEEE Transactions on Geoscience and Remote Sensing*, GE-19(3):143–152.

Braden, H. (1982). Simulationsmodell für den Wasser-, Energie- und Stoffhaushalt in Pflanzenbeständen. *Rep. Inst. Meteorol. Uni. Hannover*, (23).

Cescatti, A. (1997). Modelling the radiative transfer in discontinuous canopies of asymmetric crowns. I. Model structure and algorithms. *Ecological Modelling*, 101(2):263–274.

Clapp, R. B. and Hornberger, G. (1978). Empirical equations for some soil hydraulic properties. *Water Resource Research*, 14:601–604.

Deardorff, J. W. (1978). Efficient prediction of ground surface temperature and moisture with inclusionof a layer of vegetation. *J. Geophys. Research*, 83:1889–1903.

Goudriaan, J. (1977). *Crop Micrometeorology: A Simulation Study*. PhD thesis, Pudoc, Wageningen.

Gross, G. (2012). Numerical simulation of greening effects for idealised roofs with regional climate forcing. *Meteorologische Zeitschrift*, pages 173–181.

Heusinger, J. and Weber, S. (2017). Surface Energy Balance of an Extensive Green Roof as Quantified by Full Year Eddy-Covariance Measurements. *Science of The Total Environment*, 577:220–230.

Huttner, S. (2012). *Further Development and Application of the 3D Microclimate Simulation ENVI-met*. PhD thesis, Johannes Gutenberg-University Mainz.

Kuchling, H. (1991). *Taschenbuch der Physik*. Fachbuchverlag Leipzig- K"oln, Leipzig.

Manso, M., Teotónio, I., Silva, C. M., and Cruz, C. O. (2021). Green roof and green wall benefits and costs: A review of the quantitative evidence. *Renewable and Sustainable Energy Reviews*, 135:110111.

Mihailović, A. and Rajković, A. (1994). Impact of differently designed evaporation schemes on variability of bownratio and ground temperature in land-air parameterization modeling. *Meteorologische Zeitschrift (n.F.)*, 3:312–318.

Naot, O. and Mahrer, Y. (1989). Modelling microclimate environments: A verification study. *Boundary Layer Meteorology*, 46:333–354.

Nilson, T. (1971). A theoretical analysis of the frequency of gaps in plant stands. *Agricultural Meteorology*, 8:25–38.

Oosterlee, J. A. (2013). Green walls and building energy consumption. Master's Thesis, Eindhoven.

Pedruzo-Bagazgoitia, X., Ouwersloot, H. G., Sikma, M., van Heerwaarden, C. C., Jacobs, C. M. J., and Vilà-Guerau de Arellano, J. (2017). Direct and Diffuse Radiation in the Shallow Cumulus–Vegetation System: Enhanced and Decreased Evapotranspiration Regimes. *Journal of Hydrometeorology*, 18(6):1731–1748.

Perini, K. and Rosasco, P. (2013). Cost Benefit Analysis for Green Facades and Living Wall Systems. *Building and Environment*, 70:110–121.

Sailor, D. J. (2008). A green roof model for building energy simulation programs. *Energy and Buildings*, 40(8):1466–1478.

Schilling, V. K. (1990). A paramerization for modelling the meteorological effects of tall forests–A case study of a large clearing. *Boundary Layer Meteorology*, 55:283–304.

Simon, H. (2016). *Modeling Urban Microclimate: Development, Implementation and Evaluation of New and Improved Calculation Methods for the Urban Microclimate Model ENVI-Met*. PhD thesis, Johannes Gutenberg-University Mainz, Mainz, Germany.

Simon, H., Sinsel, T., and Bruse, M. (2020). Introduction of Fractal-Based Tree Digitalization and Accurate In-Canopy Radiation Transfer Modelling to the Microclimate Model ENVI-met. *Forests*, 11(8):869.

Simon, H., Sinsel, T., and Bruse, M. (2021). Advances in Simulating Radiative Transfer in Complex Environments. *Applied Sciences*, 11(12):5449.

Spitters, C., Toussaint, H., and Goudriaan, J. (1986). Separating the diffuse and direct component of global radiation and its implications for modeling canopy photosynthesis Part I. Components of incoming radiation. *Agricultural and Forest Meteorology*, 38(1-3):217–229.

Tjernström, M. (1989). Some tests with a surface energy balance scheme including a bulk parameterizationfor vegetation in a mesoscale model. *Boundary Layer Meteorology*, 48:33–68.